NASA TECHNICAL MEMORANDUM

UB
NASA TM X-1160

UB
NASA TM X-1160

FULL-SCALE WIND-TUNNEL INVESTIGATION OF THE AERODYNAMIC CHARACTERISTICS OF THE HL-10 MANNED LIFTING ENTRY VEHICLE

by George M. Ware

Langley Research Center
Langley Station, Hampton, Va.

NATIONAL AERONAUTICS AND SPACE ADMINISTRATION • WASHINGTON, D. C. • OCTOBER 1965

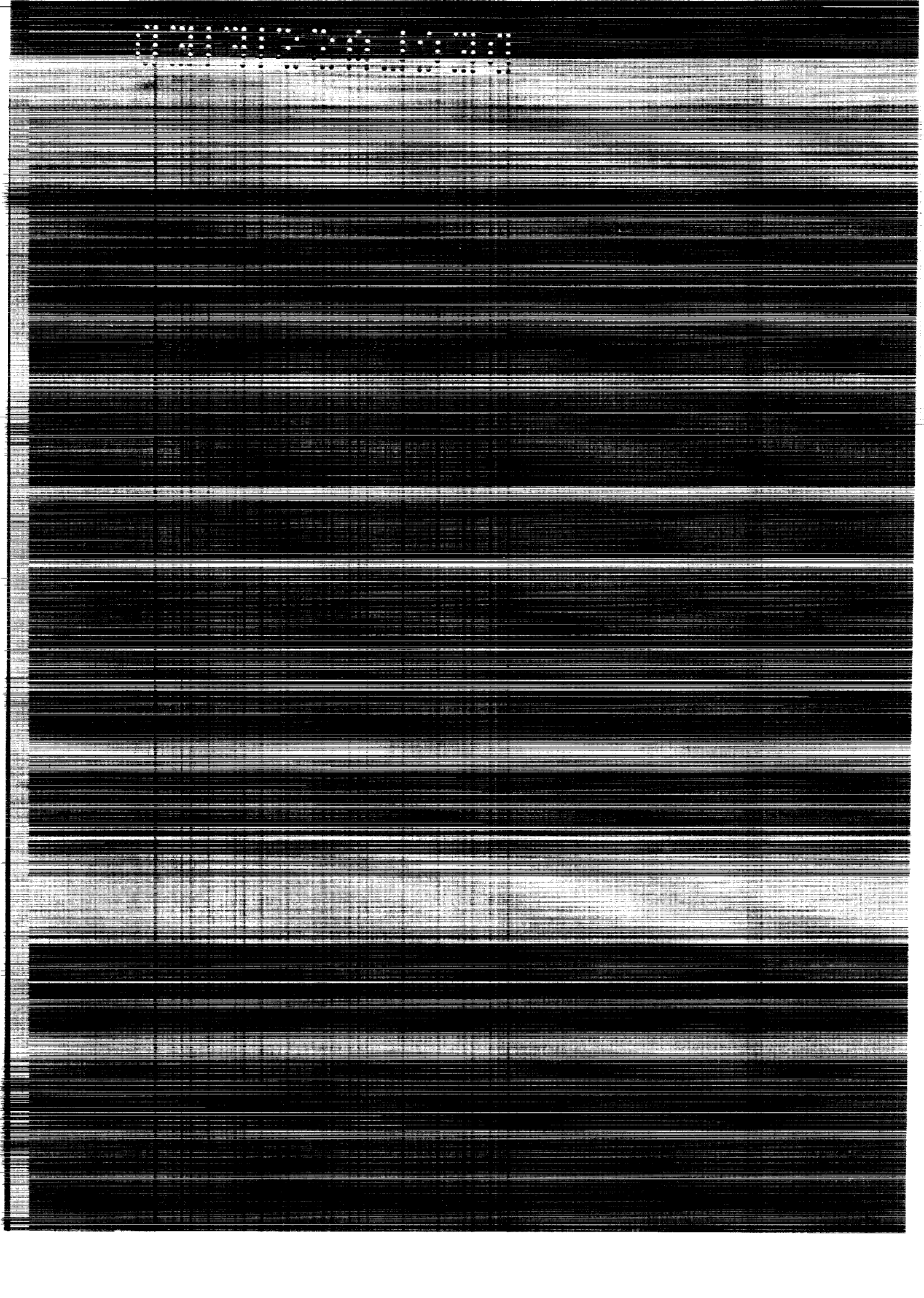

NASA TM X-1160

FULL-SCALE WIND-TUNNEL INVESTIGATION OF THE AERODYNAMIC CHARACTERISTICS OF THE HL-10 MANNED LIFTING ENTRY VEHICLE

By George M. Ware

Langley Research Center
Langley Station, Hampton, Va.

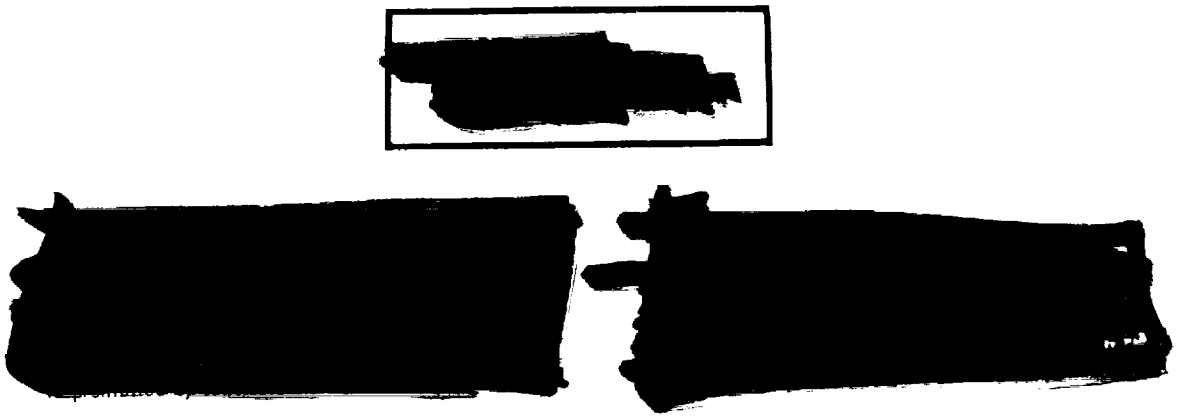

NATIONAL AERONAUTICS AND SPACE ADMINISTRATION

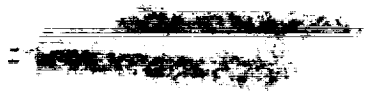

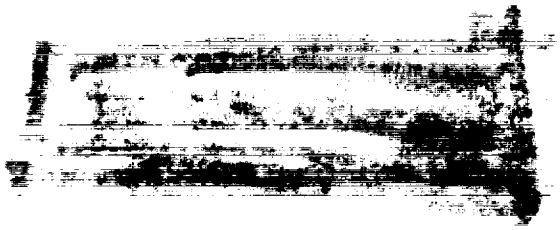

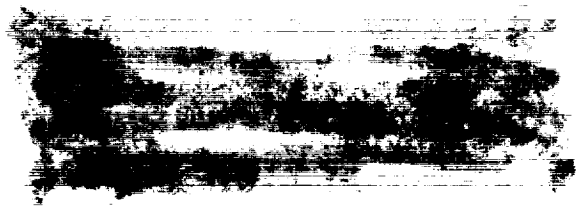

[redacted] UNCLASSIFIED

FULL-SCALE WIND-TUNNEL INVESTIGATION OF THE AERODYNAMIC CHARACTERISTICS OF THE HL-10 MANNED LIFTING ENTRY VEHICLE*

By George M. Ware
Langley Research Center

SUMMARY

An investigation has been made of the static longitudinal stability and static longitudinal and lateral control characteristics of a large-scale model of the HL-10 manned lifting entry vehicle. Configurations studied in the investigation included the body alone, the body plus center fin, and the body plus center and tip fins.

The studies showed that the stability and control characteristics of the model were satisfactory over the test angle-of-attack range. The tip fins had a large effect on the model characteristics since they greatly increased both the longitudinal stability and lift-curve slope and reduced the ratio of yawing moment to rolling moment produced by aileron deflection. The trimmed lift-drag ratio of the model with both center and tip fins was increased from 3.4 to 4.7 by boattailing the fins, rudder, and elevons.

INTRODUCTION

The National Aeronautics and Space Administration is conducting a number of wind-tunnel investigations to provide aerodynamic data from hypersonic to low-subsonic speeds for the HL-10 manned lifting entry vehicle. The studies (for example, refs. 1 to 16) are aimed at developing a lifting-body configuration which will possess adequate longitudinal and lateral stability and control over the speed and angle-of-attack ranges with a hypersonic lift-drag ratio of about 1.0 and a subsonic lift-drag ratio sufficiently high to allow a conventional glide landing.

The present force-test investigation was made with a 28-foot (8.53 meter) model of the HL-10 to provide low-speed aerodynamic information at fairly high Reynolds numbers. The model was tested with a center- plus tip-fin arrangement which was shown in previous investigations to be necessary for directional

*Title, Unclassified.

[redacted]

stability over the speed range and with a boattailed version of this three-fin configuration which was suggested in reference 12 as a means of improving subsonic performance. Data are also presented for the body alone and the body with a center fin. The tests were conducted over an angle-of-attack range from 0° to about 34°.

SYMBOLS

The lateral data are referred to the body system of axes and the longitudinal data are referred to the wind axes. (See fig. 1.) The origin of the axes was located to correspond to a longitudinal center-of-gravity position at 53 percent of the body length and 1.25 percent of the body length below the model reference line. The coefficients are based on a planform area of 280 square feet (26 square meters), a body length of 28 feet (8.53 meters), and a span of 18 feet (5.49 meters).

C_D	drag coefficient
C_h	hinge-moment coefficient
C_L	lift coefficient
ΔC_l	incremental rolling-moment coefficient
C_m	pitching-moment coefficient
ΔC_n	incremental yawing-moment coefficient
ΔC_Y	incremental side-force coefficient
D	drag
F_Y	side force
L	lift
L/D	lift-drag ratio
M_X	rolling moment
M_Y	pitching moment
M_Z	yawing moment
R	Reynolds number
X,Y,Z	body reference axes

α angle of attack, degrees

β angle of sideslip, degrees

δ_a aileron deflection, $\delta_{e,R} - \delta_{e,L}$, degrees

δ_e elevator deflection, positive with trailing edge down, degrees

$\delta_{e,R}$ right elevator deflection, positive with trailing edge down, degrees

$\delta_{e,L}$ left elevator deflection, positive with trailing edge down, degrees

δ_r rudder deflection, positive with trailing edge deflected left, degrees

θ angular difference between upper surfaces of original and modified elevons, degrees

APPARATUS AND MODEL

The tests were conducted in the Langley full-scale tunnel which has a 30- by 60-foot (9.14 by 18.28 meters) open-throat test section and is capable of speeds up to about 95 knots. A complete description of the tunnel and test apparatus may be found in reference 17. Photographs of the model mounted for force tests in the tunnel are presented in figure 2, and drawings of the model are presented in figure 3. The model had a 74° delta planform with a thick negatively cambered airfoil section. It was tested with several different fin arrangements - specifically, a center fin designated E_2 (fig. 3(a)), a center fin E_2 plus tip fins designated I_4 (fig. 3(b)), and a boattailed three-fin configuration designated modified fins E_2 plus I_4 (fig. 3(c)). Auxiliary drawings of the model with fins I_4 are presented in figure 3(d) to define more clearly the toe-in and roll-out angles of the tip fins.

The modified three-fin configuration was tested with boattailed elevon surfaces. The various elevon configurations are identified in terms of the angular difference between the upper surfaces of the original and modified elevon, measured parallel to the model center line. (See fig. 3(c).) The modified three-fin configuration had boattailed elevons with $\theta = 4^\circ$ unless otherwise noted. This configuration was also equipped with speed brakes. The speed brakes are split surfaces, mounted on the modified center fin, that move together as a rudder or open up to act as brakes. For convenience in presentation, the landing gear used in the investigation is shown in figure 3(b) mounted on the three-fin configuration although the test was actually conducted with the landing gear on the body alone.

TESTS

Static force tests were made to determine the static longitudinal stability and static longitudinal and lateral control characteristics of the body alone, the body with a center vertical fin, and the body with a center vertical fin plus tip fins over an angle-of-attack range from 0° to about 34°. Tests were also made to determine the effect of boattailing the fins and elevon surfaces on the longitudinal characteristics of the model. The investigation included measurements of the elevon hinge moments. The tests were made at velocities of about 51 and 79 knots which correspond to Reynolds numbers, based on the model length of 28 feet (8.53 meters), of approximately 15×10^6 and 24×10^6, respectively.

The force and moment data presented have been corrected for airstream-misalinement, jet-boundary, buoyancy, and blockage effects.

RESULTS AND DISCUSSION

Longitudinal Stability and Control Characteristics

Effect of Reynolds number.- Although a rather large model was used in the investigation it was still impossible to duplicate the flight Reynolds number that will be encountered by the HL-10 vehicle during approach and landing because of limiting maximum tunnel airspeed. In order to establish whether variation in Reynolds number had an appreciable effect over the range of velocities of which the tunnel is capable, a few tests were made near maximum speed and at about half speed. The results of these tests are presented in figure 4 for the body alone and for the complete model with modified fins. The data of figure 4(a) show that variations in Reynolds number from 15×10^6 to 24×10^6 have no appreciable effect on the characteristics of the body alone. The data for the modified fin configuration (fig. 4(b)) show only very small differences in the model characteristics with Reynolds number. Specifically, they show that the variation of the lift and pitching moment with angle of attack was somewhat more linear for the higher Reynolds number and that the model had a slightly higher untrimmed maximum lift-drag ratio at the higher Reynolds number. These data indicate that the fins or fin junctures were somewhat more sensitive to changes in Reynolds number than was the body itself. The effects of Reynolds number were considered sufficiently small, however, to be of no practical significance, and therefore the remaining tests were made at the lower speed where tests were easier to make.

Effect of fin configuration.- The effect of fin configuration on the longitudinal characteristics of the model is presented in figure 5. These data show that the body alone was longitudinally stable about its design center-of-gravity position and that the stability level increased significantly above an angle of attack of about 20°. Addition of the center fin E_2 to the body had little effect on lift and pitching moment but did add an increment of drag with

resulting loss in maximum lift-drag ratio. It may also be noted that the model in this configuration with an elevator deflection of 0° was trimmed at maximum L/D. Addition of tip fins I_4 to the body—center-fin configuration had a large effect on the characteristics of the model. There was an increase in lift and lift-curve slope and a large increase in longitudinal stability up to an angle of attack of about 20°, evidently because of an end-plate effect of the tip fins. This increase in stability, which made the pitching-moment variation with angle of attack more linear over the test range, shifted the longitudinal trim point to a much lower angle of attack. As might be expected, the addition of the tip fins also increased the drag of the configuration. The increases in both lift and drag were compensating, from the standpoint of lift-drag ratio, as seen from the fact that the untrimmed lift-drag ratios of the model with fin E_2 or fins E_2 plus I_4 were the same. In order to improve the low-speed lift-drag characteristics of the three-fin configuration, the fins and elevon surfaces were boattailed (see fig. 3(c)) as suggested by the small-scale model tests presented in reference 12. These modifications had almost no effect on lift but reduced the drag of the model and therefore significantly increased the maximum untrimmed lift-drag ratio. The pitching-moment characteristics of the three-fin configuration were relatively unchanged, however, and the value of maximum L/D occurred well off trim conditions.

Effect of elevon trailing-edge thickness.- The small-scale subsonic tests of the HL-10 reported in reference 12 indicated that some of the increase in lift-drag ratio resulted from boattailing the elevon surfaces. Therefore, the present investigation included a few tests with $\delta_e = 0^\circ$ to determine the effect of the amount of elevon boattailing. In these tests the elevon was boattailed 0°, 4°, 8°, and 12°. (See fig. 3(c).) The data presented in figure 6 show that decreasing the trailing-edge thickness in the manner described had the same effect on the lift and pitching moment as a positive elevator deflection. The data also indicate that boattailing the elevon caused a small increase in maximum untrimmed lift-drag ratio with the highest value of L/D occurring for the boattail angle of 4°. Larger boattail angles did not increase L/D because the upper surface of the elevon stalled at an angle of attack of 0°. In unpublished results from small-scale tests made in the Langley high-speed 7- by 10-foot tunnel, however, where trim conditions were determined for the various amounts of elevon boattail, the highest trimmed L/D occurred with the maximum amount ($\theta \approx 12^\circ$) of boattail.

Trim characteristics.- The effect of elevator deflection on the longitudinal characteristics of the body alone and of the body with various fin configurations are presented in figure 7. These data show that, in general, the effectiveness of the elevators was maintained over the test angle-of-attack range although there was some loss in effectiveness for some configurations at the extreme elevator deflections, evidently because of stalling of the surfaces. The elevator was more effective with tip fins on than with them off, and the variation of the lift and pitching-moment curves appeared to be more linear except for positive elevator deflections.

The data of figure 7 have been summarized in figure 8 in the form of the longitudinal trim characteristics for each of the configurations tested.

Although the data of figures 5 and 7 show that the tip fins caused a large increase in lift-curve slope and, therefore, untrimmed lift for a given angle of attack, trimming out the pitching moment produced by these fins resulted in about the same trimmed lift characteristics as indicated in figure 8 for the model regardless of fin configuration. The trimmed drag value, however, varied by a considerably larger percentage between configurations. The major change was the reduction in drag with the change from the original to the modified three-fin configuration. This reduction resulted in an increase in maximum trimmed lift-drag ratio from about 3.4 for the model with fins E_2 plus I_4 to about 4.7 for the modified three-fin model. The maximum trimmed values of L/D for the body alone and the body with center fin E_2 were about 4.3 and 3.9, respectively.

Effect of speed brakes.- The effect of symmetrical deflection angles of 0°, 20°, and 40° of the speed brakes on the longitudinal characteristics of the modified three-fin configuration may be seen in figure 9. The data show that the speed brakes not only produced the desired increase in drag but reduced the lift and caused a large trim change because of the pitching moment introduced. The maximum deflection angle shifted the trimmed angle of attack for $\delta_e = -10°$ from about 12° to 24° and reduced the trimmed L/D from about 4.0 to 2.7.

Effect of landing gear.- The effects of extending the landing gear on the longitudinal characteristics of the body alone are shown in figure 10(a). The landing-gear-extended data in figure 10(b) were obtained by taking incremental values between body alone and body plus landing gear from figure 10(a) and adding them to values for the modified configuration with gear retracted. These data are representative of a landing-gear-doors-closed configuration. The data show that the gear had little effect on the lift and produced only a small negative pitching moment but greatly increased the drag and consequently caused a large decrease in the untrimmed L/D.

Elevator hinge moments.- The variation of the elevator hinge moments with angle of attack is shown in figure 11 for several elevator deflections with tip fins off and on. The data show that with tip fins on the hinge-moment curves are steeper as might be expected because of the end-plate effect of the tip fins which also resulted in an increase in lift-curve slope as pointed out previously.

Lateral Control Characteristics

Small-scale model tests of the configuration with fin E_2 (ref. 11) and unpublished data (obtained in the Langley 8-foot transonic pressure tunnel and the Langley high-speed 7- by 10-foot tunnel) of the model with the basic and modified fins E_2 plus I_4 have indicated that these configurations have satisfactory lateral stability. Because of this fact, and because of the difficulty and time required to make sideslip changes in the full-scale tunnel, no lateral stability tests were made. The lateral control characteristics of the 28-foot (8.53 meter) model, however, were investigated at an angle of sideslip of 0°.

[redacted]

Rudder effectiveness.- The rudder effectiveness as determined for the model with fins E_2, E_2 plus I_4, and modified E_2 plus I_4 is given in figure 12. (The rudder was located only on fin E_2.) The data show that the rudder deflection produced relatively constant yawing-moment increments over the angle-of-attack range and rather sizable adverse rolling-moment increments. It is also seen that deflecting the rudder from -20° to -45° (figs. 12(a) and (b)) provided very little additional yawing moment. In the case of the modified configuration (fig. 12(c)), it can be seen that most of the yawing moment was produced by only 10° of rudder deflection. In order to compare the effectiveness of the rudders more directly, the curves in figure 12 for the condition of $\delta_r = -20°$ for the three configurations were repeated in figure 13. The rudder was somewhat more effective with tip fins off than with them on - evidently because deflecting the rudder caused a change in the tip-fin load that introduced a yawing moment to oppose that of the rudder. Boattailing the rudder to form the modified fin E_2 reduced its effectiveness for the given 20° deflection. It was noted, however, that the windward surface of the boattailed rudder had 9° less angle to the free stream than did the original rudder. This condition raised the question of whether a "dead" spot might exist in the control characteristics for rudder deflection near 0°. The cross plot of the modified-rudder data (fig. 14), however, indicates that there was no loss in control effectiveness at low deflection angles but that there was some loss in effectiveness above $\delta_r = -10°$ - probably because of flow separation over the downwind surface.

Aileron effectiveness.- The aileron effectiveness for the various configurations studied is presented in figure 15 for several aileron deflections and trim elevator settings. The data show decided nonlinearities which are attributed to flow separation on the more highly deflected elevon. The influence of the tip fins on the effectiveness of the aileron is seen in figure 16 where data from figure 15 are summarized for the same aileron and elevator deflections. The ailerons produce about twice as much incremental rolling moment with tip fins on as with tip fins off. This increase is attributed, as was the increase in elevator effectiveness, to the end-plate effect of the tip fins. Aileron deflection, regardless of fin configuration, produced favorable yawing moments. The ratio of yawing moment to rolling moment produced by the ailerons, however, was much higher for the model with tip fins off. This effect evidently results from part of the large favorable yawing moment produced by the center fin (due to differential pressure set up by the aileron deflection) being balanced out by unfavorable yawing moments produced by the tip fins.

CONCLUSIONS

An investigation has been made in the Langley full-scale tunnel of a 28-foot (8.53 meter) model of the HL-10. Configurations studied in the investigation included the body alone, the body plus center fin, and the body plus center and tip fins. From the results of the force-test investigation, the following conclusions are made:

[redacted]

1. The longitudinal stability and the longitudinal and lateral control characteristics of the model are satisfactory over the angle-of-attack range from 0° to about 34°.

2. The tip fins greatly altered the characteristics of the model by increasing the longitudinal stability and lift-curve slope and decreasing the ratio of yawing moment to rolling moment produced by aileron deflection.

3. Reducing the base area by boattailing the fins, rudder, and elevons increased the trimmed lift-drag ratio of the model with both center and tip fins from 3.4 to 4.7.

Langley Research Center,
National Aeronautics and Space Administration,
Langley Station, Hampton, Va., August 11, 1965.

REFERENCES

1. Johnston, Patrick J.: Stability Characteristics of a Manned Lifting Entry Vehicle at a Mach Number of 20.3 in Helium. NASA TM X-1156, 1965.

2. Harris, Julius E.: Longitudinal Aerodynamic Characteristics of a Manned Lifting Entry Vehicle at a Mach Number of 19.7. NASA TM X-1080, 1965.

3. Rainey, Robert W.; and Ladson, Charles L.: Preliminary Aerodynamic Characteristics of a Manned Lifting Entry Vehicle at a Mach Number of 6.8. NASA TM X-844, 1963.

4. Ladson, Charles L.: Aerodynamic Characteristics of a Manned Lifting Entry Vehicle at a Mach Number of 6.8. NASA TM X-915, 1964.

5. Ladson, Charles L.: Aerodynamic Characteristics of a Manned Lifting Entry Vehicle With Modified Tip Fins at Mach 6.8. NASA TM X-1158, 1965.

6. McShera, John T., Jr.; and Campbell, James F.: Stability and Control Characteristics of a Manned Lifting Entry Vehicle at Mach Numbers From 2.29 to 4.63. NASA TM X-1019, 1964.

7. Campbell, James F.; and McShera, John T., Jr.: Stability and Control Characteristics From Mach Number 1.50 to 2.86 of a Model of a Manned Lifting Entry Vehicle. NASA TM X-1117, 1965.

8. Silvers, H. Norman; and Campbell, James F.: Stability Characteristics of a Manned Lifting Entry Vehicle With Various Fins at Mach Numbers From 1.50 to 2.86. NASA TM X-1161, 1965.

9. Rainey, Robert W.; and Ladson, Charles L.: Aerodynamic Characteristics of a Manned Lifting Entry Vehicle at Mach Numbers From 0.2 to 1.2. NASA TM X-1015, 1964.

10. Ware, George M.: Aerodynamic Characteristics of Models of Two Thick 74° Delta Manned Lifting Entry Vehicles at Low-Subsonic Speeds. NASA TM X-914, 1964.

11. Ware, George M.: Effect of Fin Arrangements on Aerodynamic Characteristics of a Thick 74° Delta Manned Lifting Entry Vehicle at Low-Subsonic Speeds. NASA TM X-1020, 1965.

12. Spencer, Bernard, Jr.: An Investigation of Methods of Improving Subsonic Performance of a Manned Lifting Entry Vehicle. NASA TM X-1157, 1965.

13. Moul, Martin T.; and Brown, Lawrence W.: Some Effects of Directional Instability on Lateral Handling Qualities of an Early Version of a Manned Lifting Entry Vehicle. NASA TM X-1162, 1965.

14. Dunavant, James C.; and Everhart, Philip E.: Investigation of the Heat Transfer to the HL-10 Manned Lifting Entry Vehicle at a Mach Number of 8. NASA TM X-998, 1964.

15. Everhart, Philip E.; and Hamilton, H. Harris: Investigation of Roughness-Induced Turbulent Heating to the HL-10 Manned Lifting Entry Vehicle at a Mach Number of 8. NASA TM X-1101, 1965.

16. Rainey, Robert W.: Summary of an Advanced Manned Lifting Entry Vehicle Study. NASA TM X-1159, 1965.

17. DeFrance, Smith J.: The N.A.C.A. Full-Scale Wind Tunnel. NACA Rept. 459, 1933.

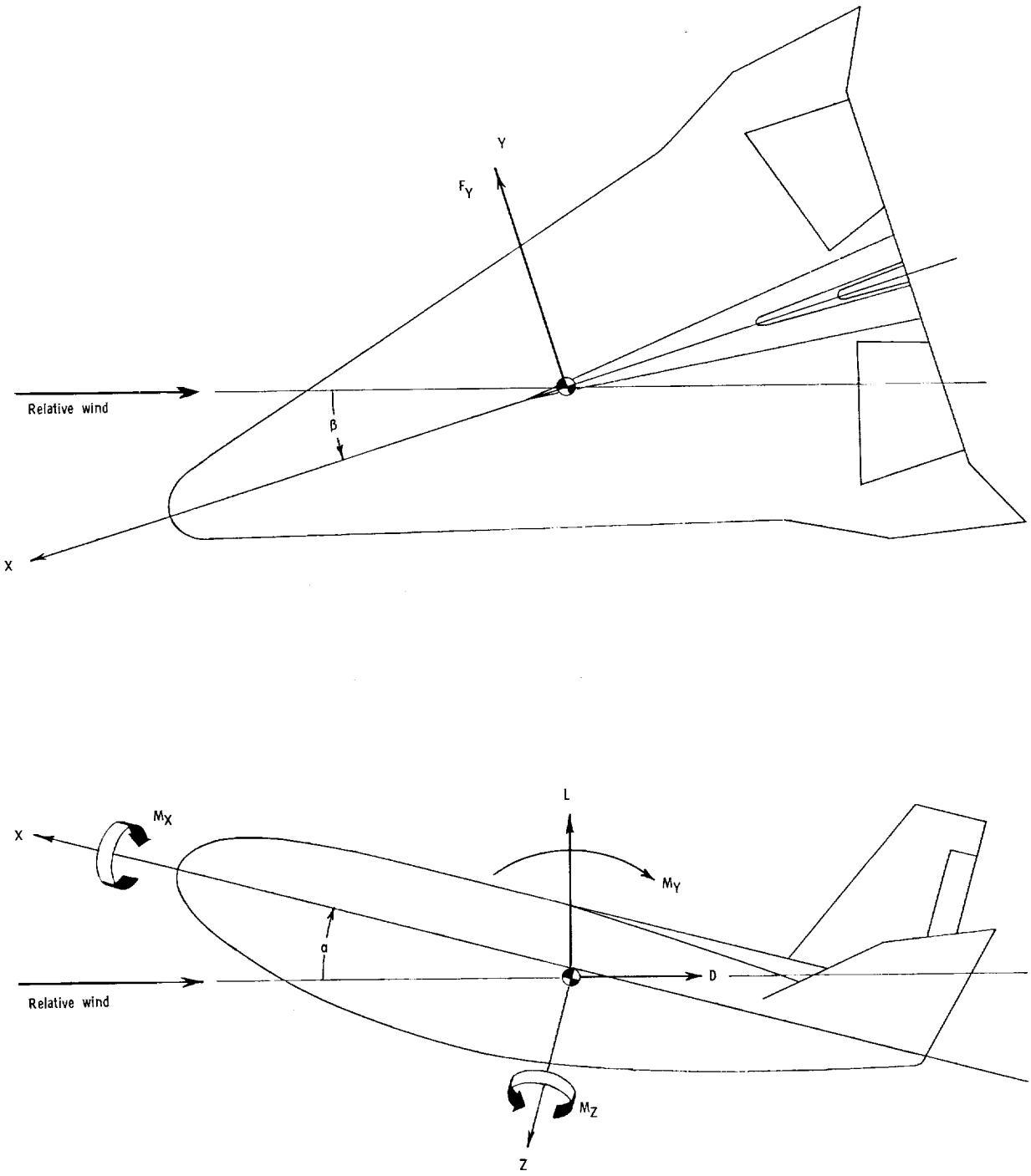

Figure 1.- System of axes used in investigation. Longitudinal data are referred to wind axes and lateral data are referred to body axes. Arrows indicate positive direction of forces, moments, and angles.

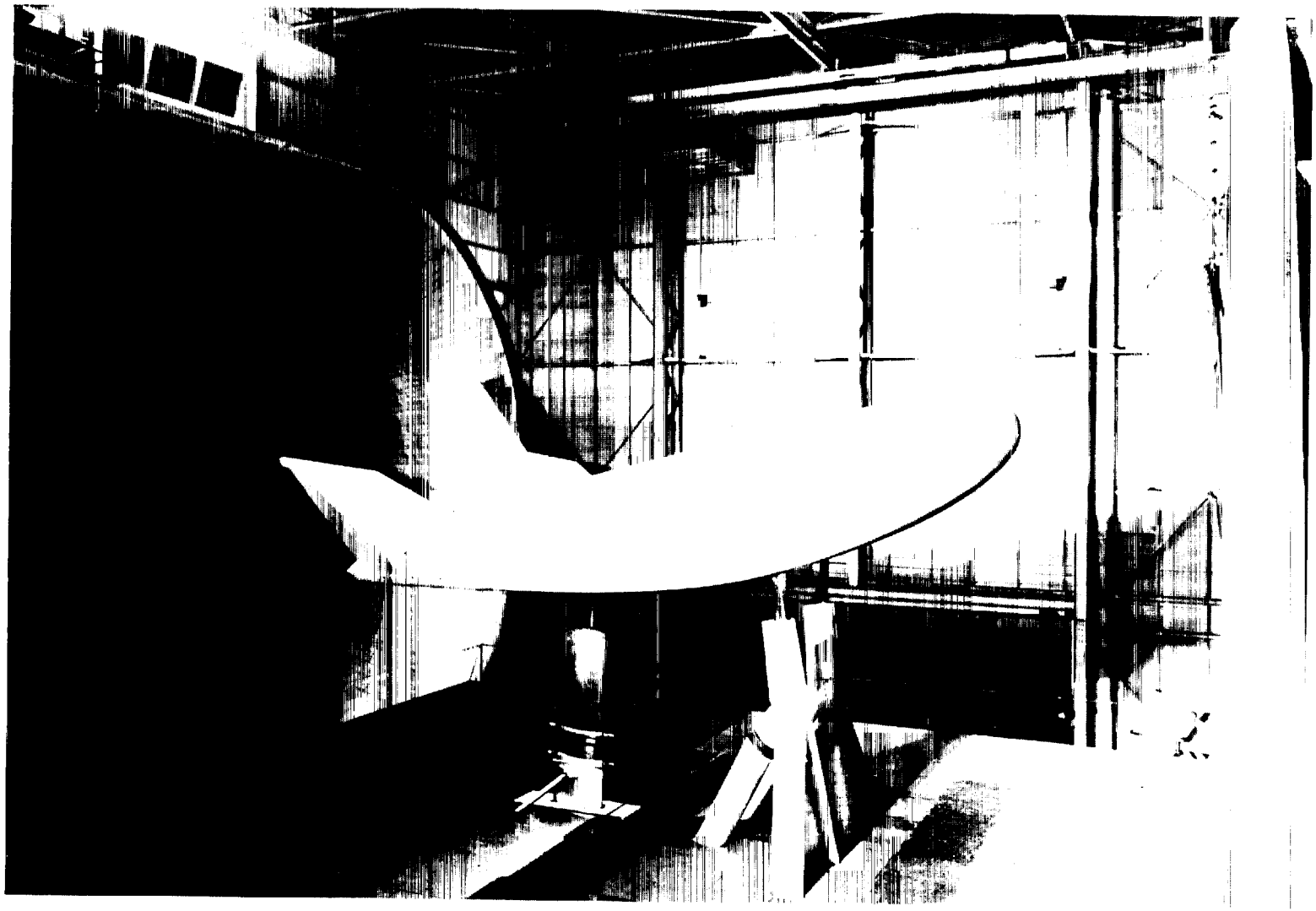

(a) Three-quarter front view showing support-system details. L-65-2437

Figure 2.- Model mounted for force testing in Langley full-scale tunnel.

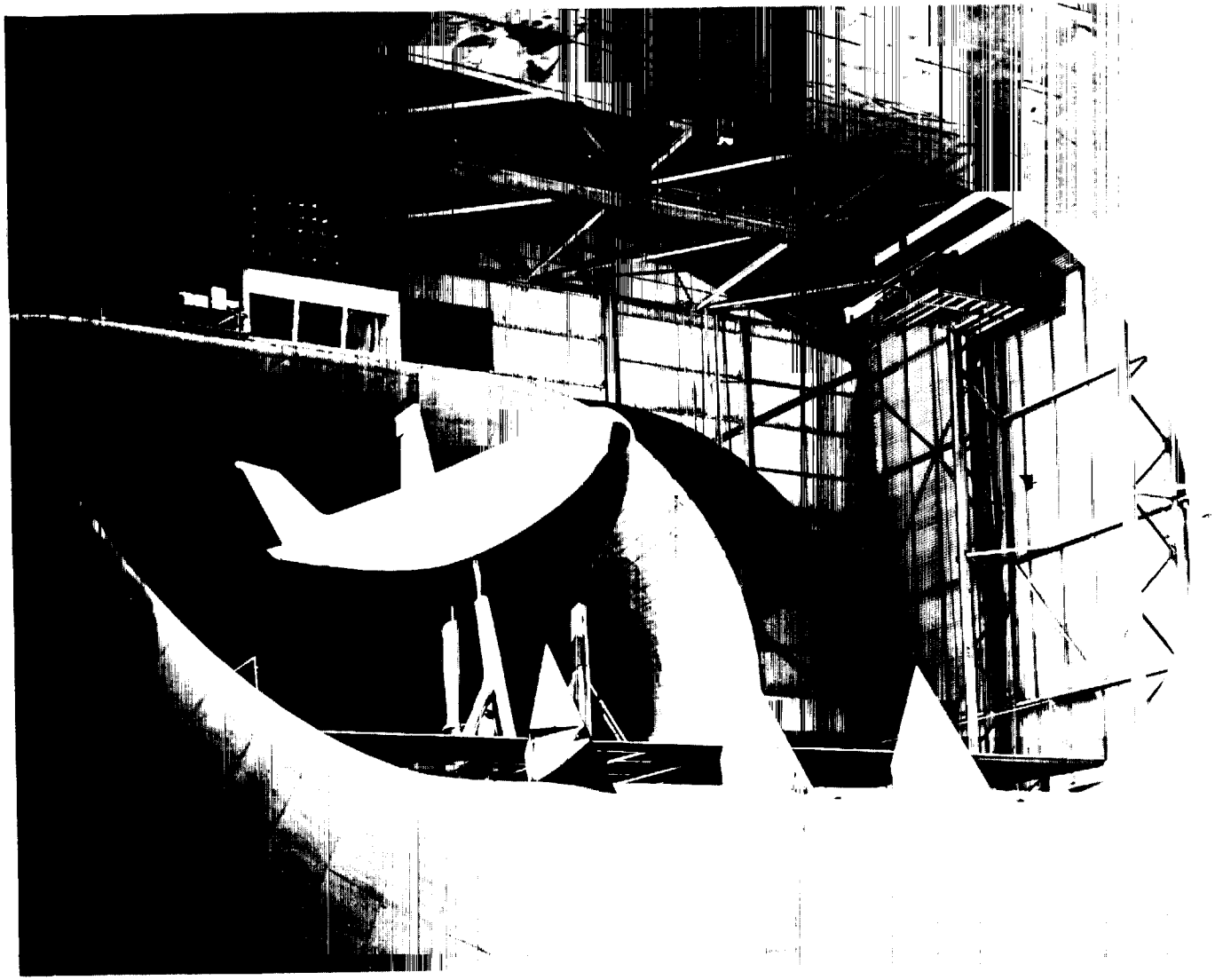

(b) View from tunnel entrance cone.

L-65-2438

Figure 2.- Concluded.

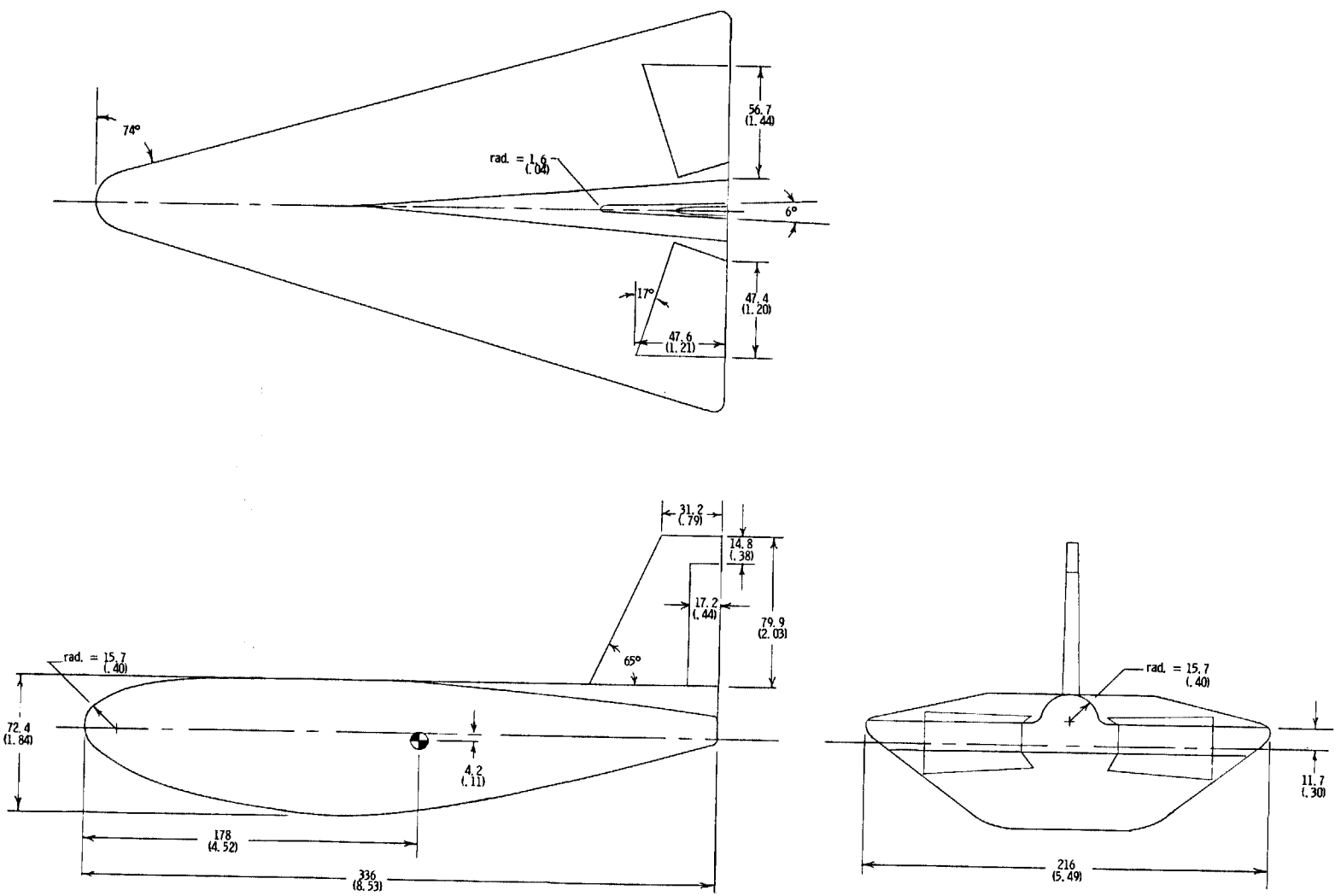

(a) Body with center fin E_2.

Figure 3.- Drawings of the model used in the investigation. Dimensions are in inches (meters).

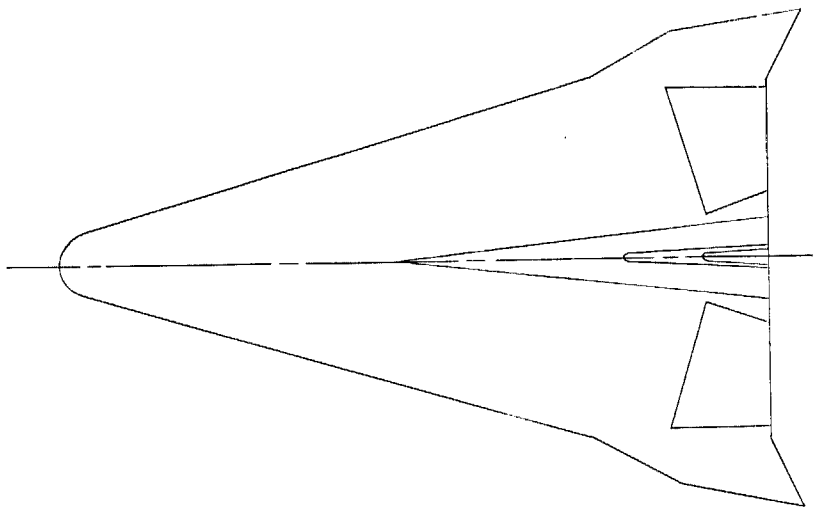

Dimensions are in plane of surface.

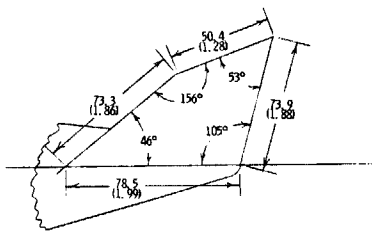

Tip fin l_4

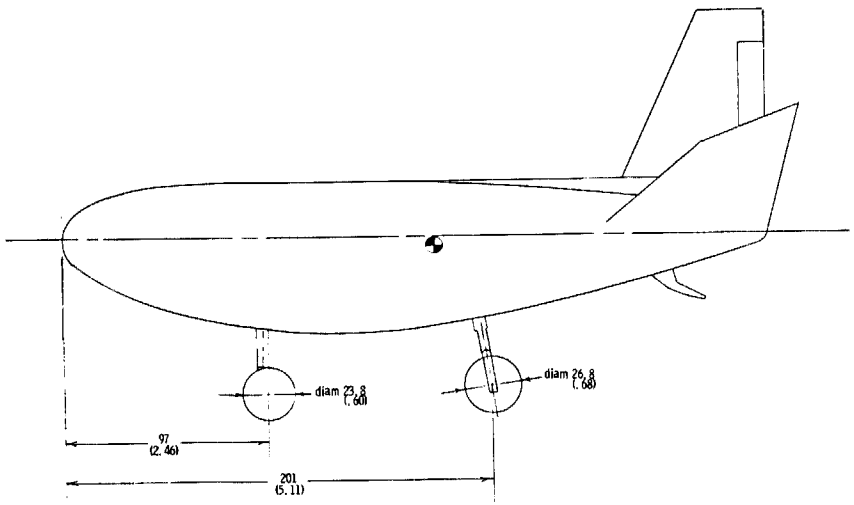

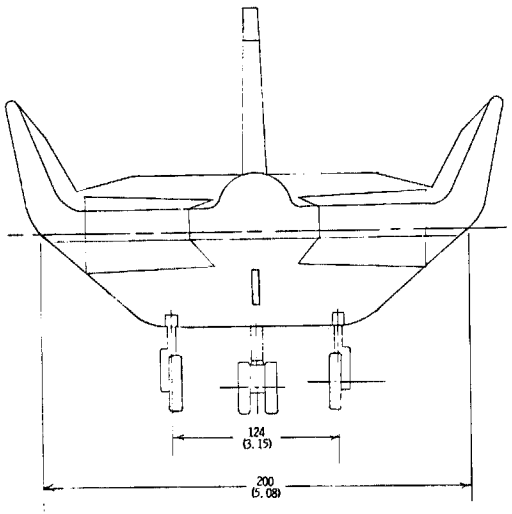

(b) Body with center fin E_2 plus tip fin l_4.

Figure 3.- Continued.

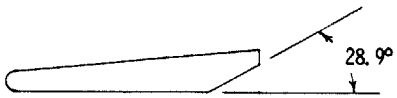

Section A-A

Section B-B

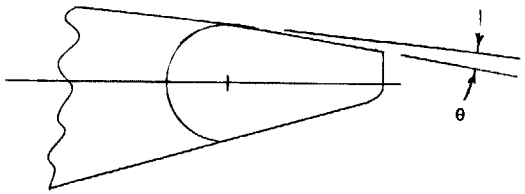

Section C-C

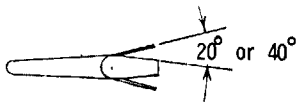

Speed-brake detail

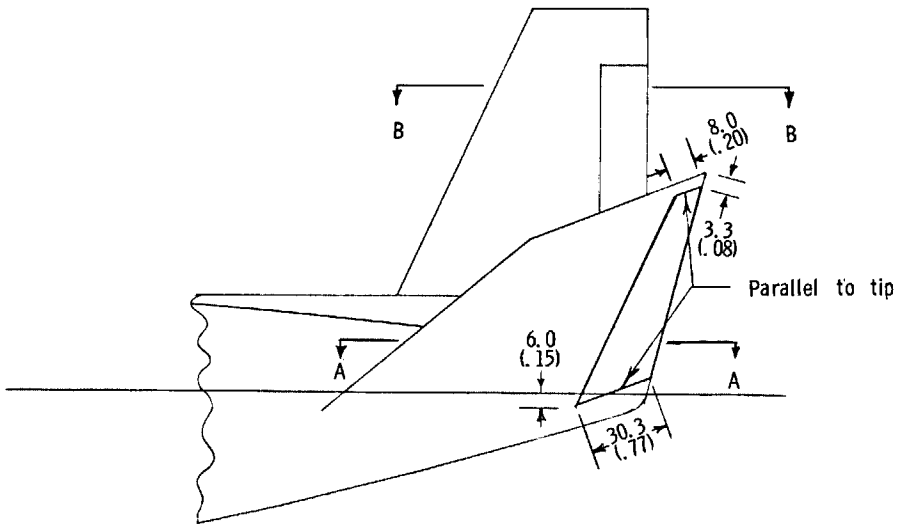

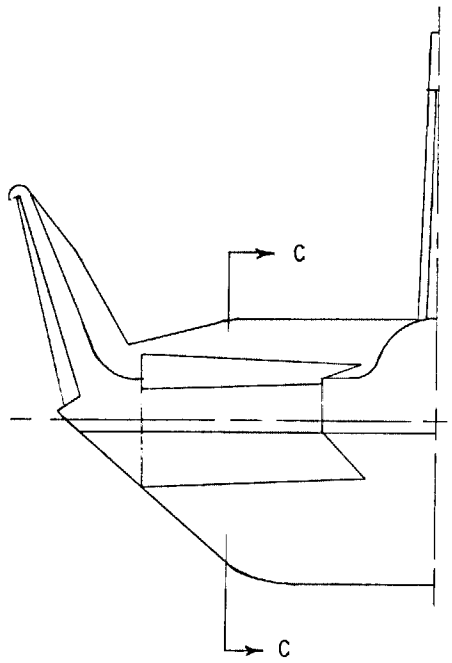

(c) Modified fins E_2 plus I_4.

Figure 3.- Continued.

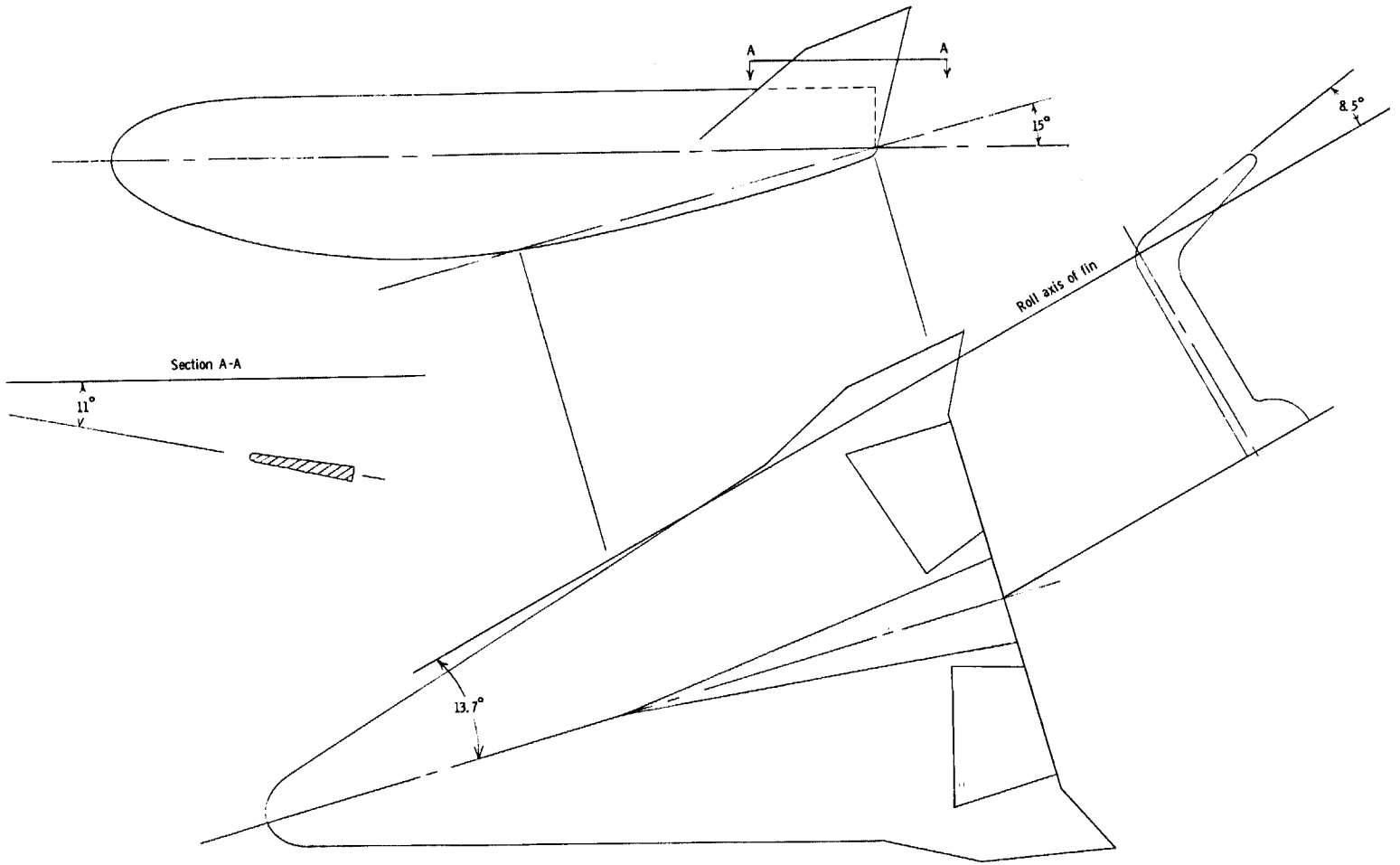

(d) Auxiliary view showing roll-out and toe-in angles of tip fin 1_4.

Figure 3.- Concluded.

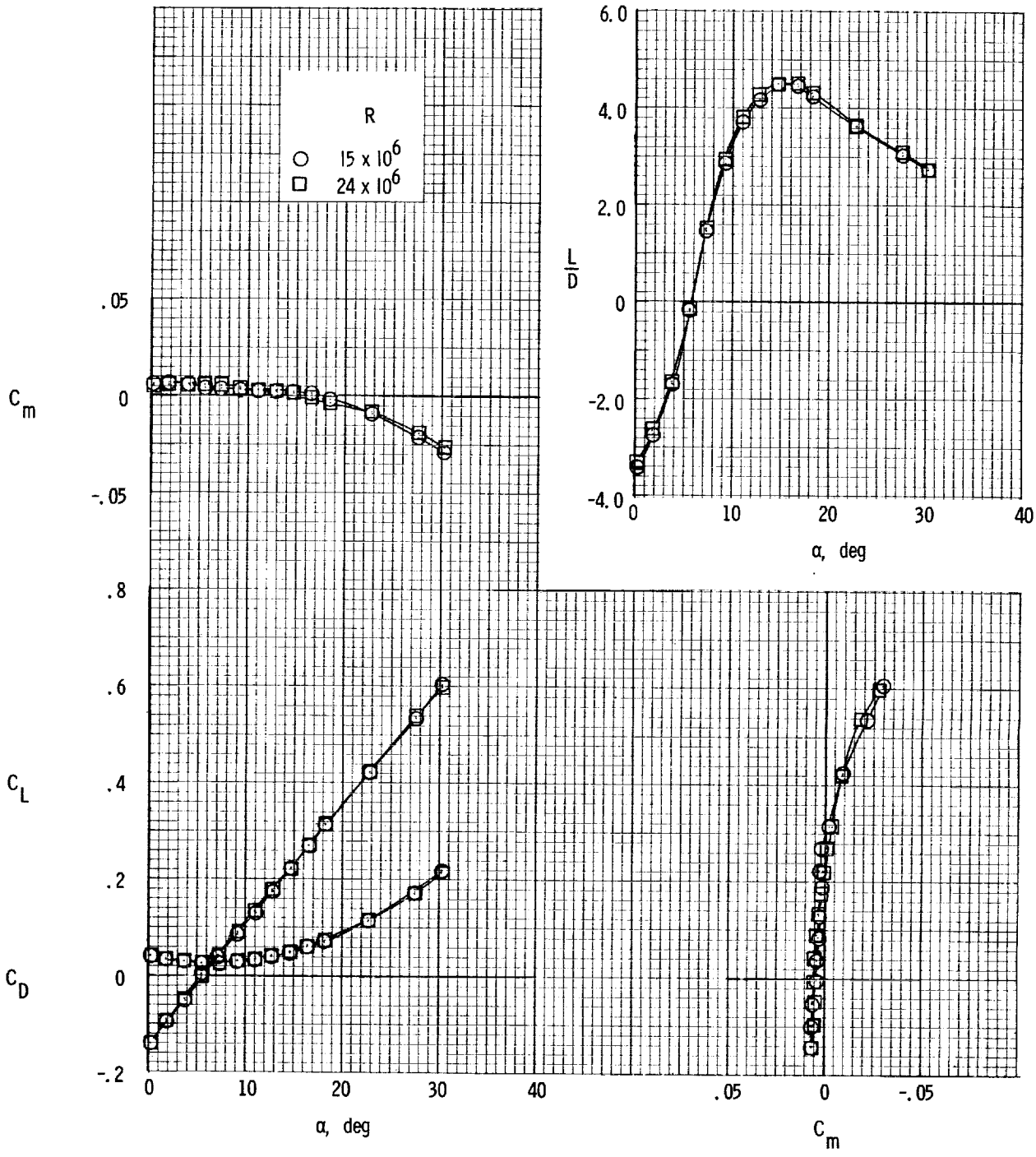

(a) Body alone. $\delta_e = 0^o$.

Figure 4.- Effect of Reynolds number on longitudinal characteristics of model.

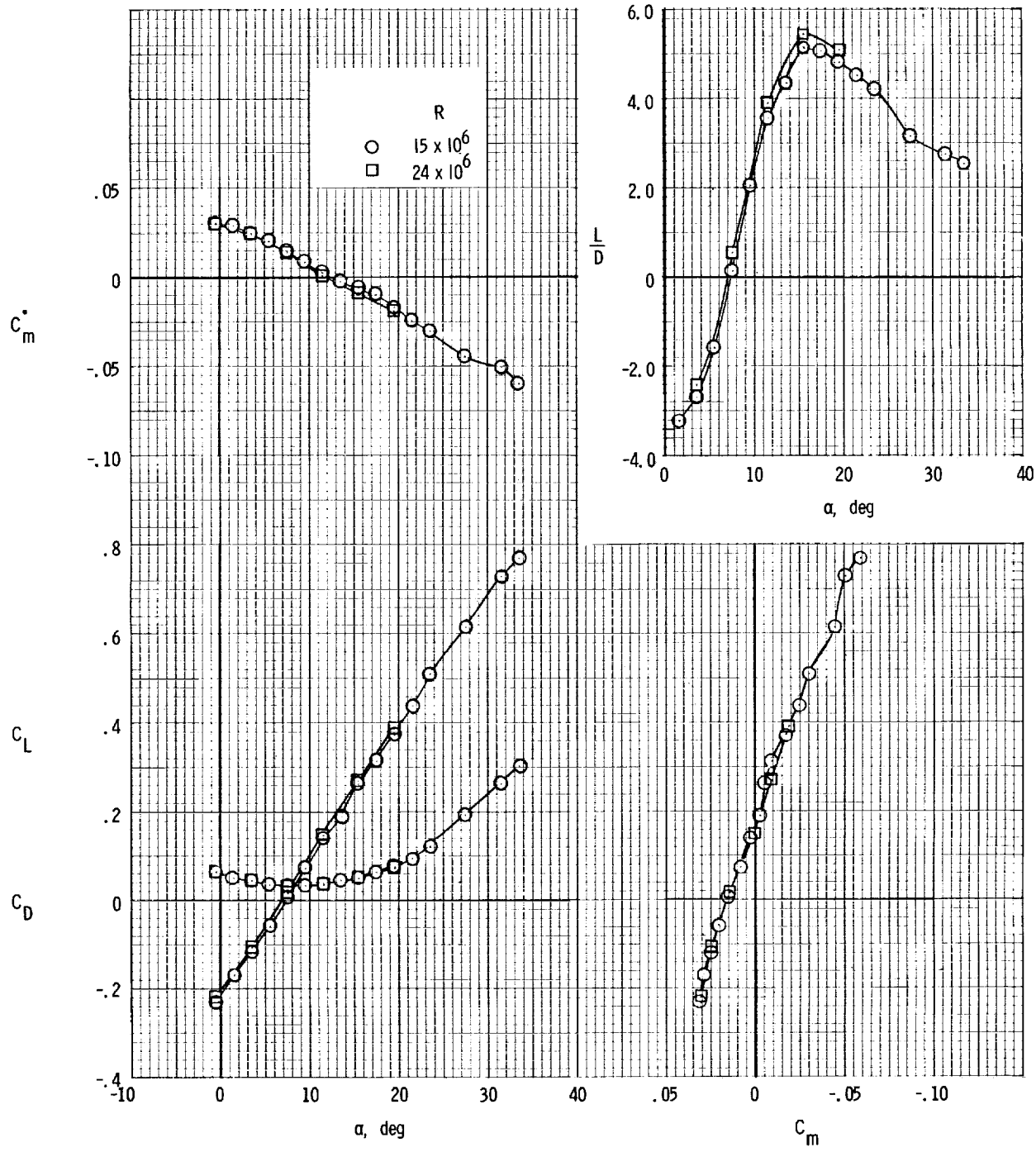

(b) Body with modified fins E_2 + I_4. $\delta_e = -10^0$; $\theta = 4^0$.

Figure 4.- Concluded.

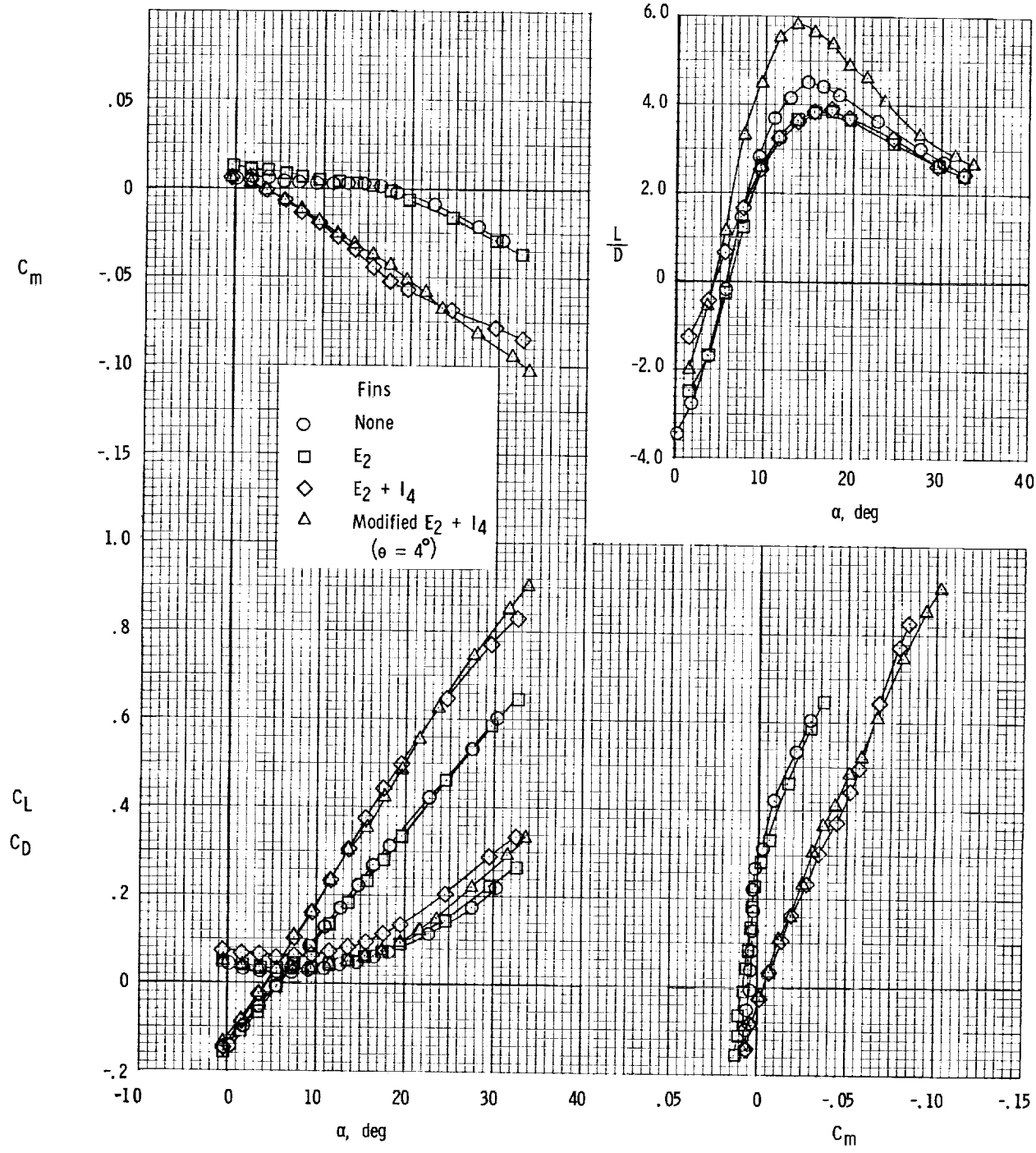

Figure 5.- Effect of fin configuration on longitudinal characteristics of model. $\delta_e = 0°$.

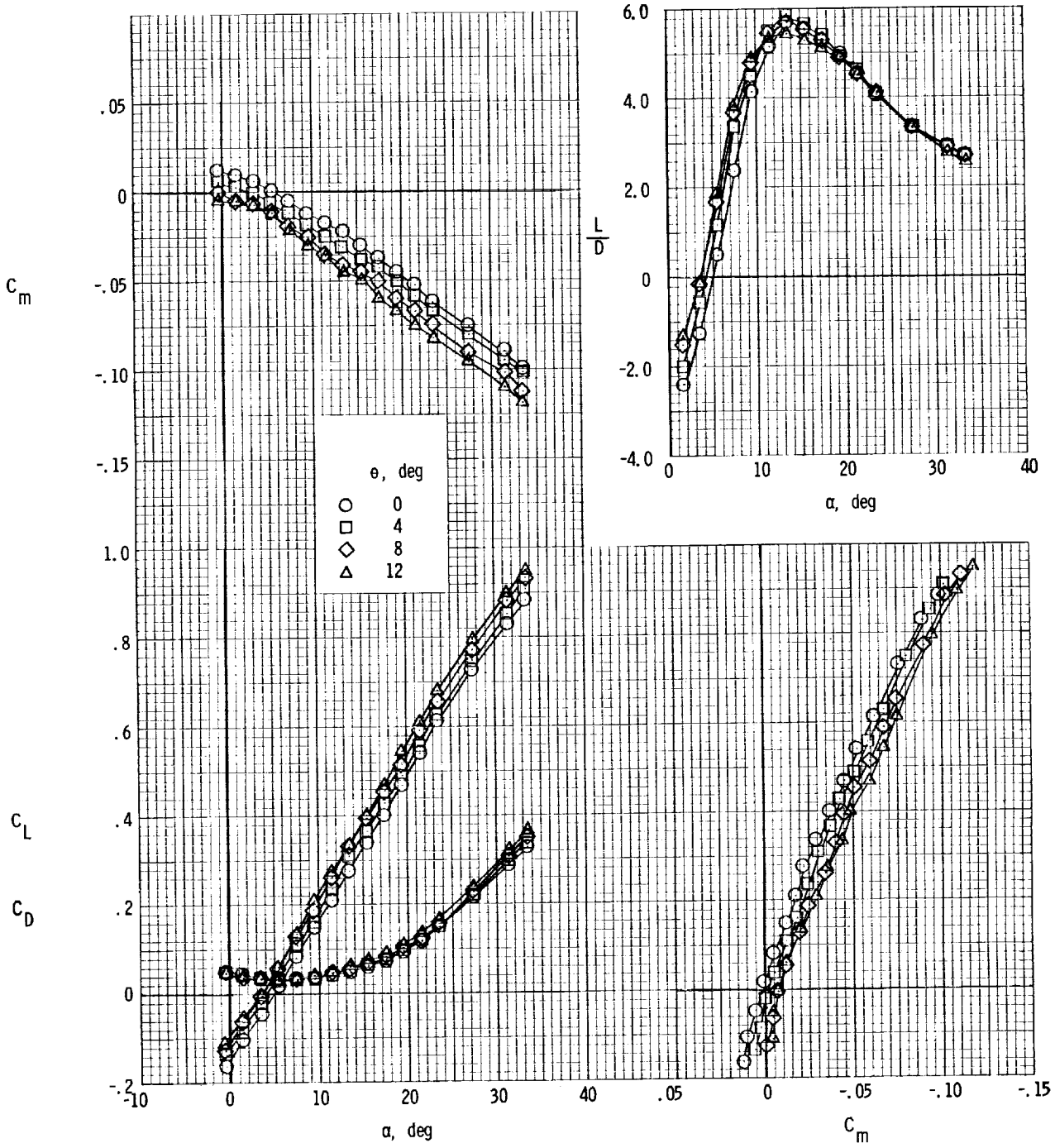

Figure 6.- Effect of elevon thickness on longitudinal characteristics of model with modified fins. $\delta_e = 0^o$.

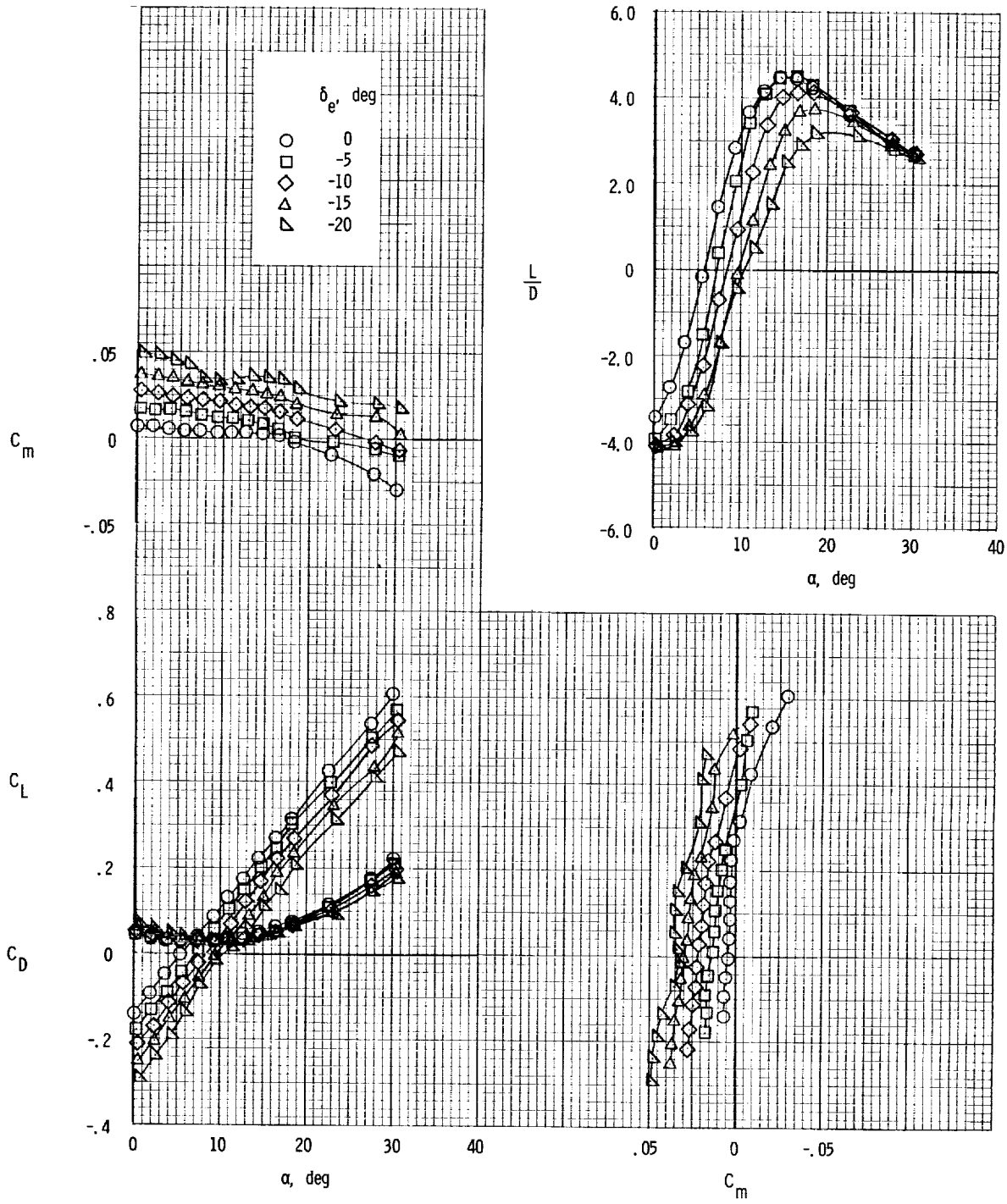

(a) Body alone.

Figure 7.- Effect of elevator deflection on longitudinal characteristics of model.

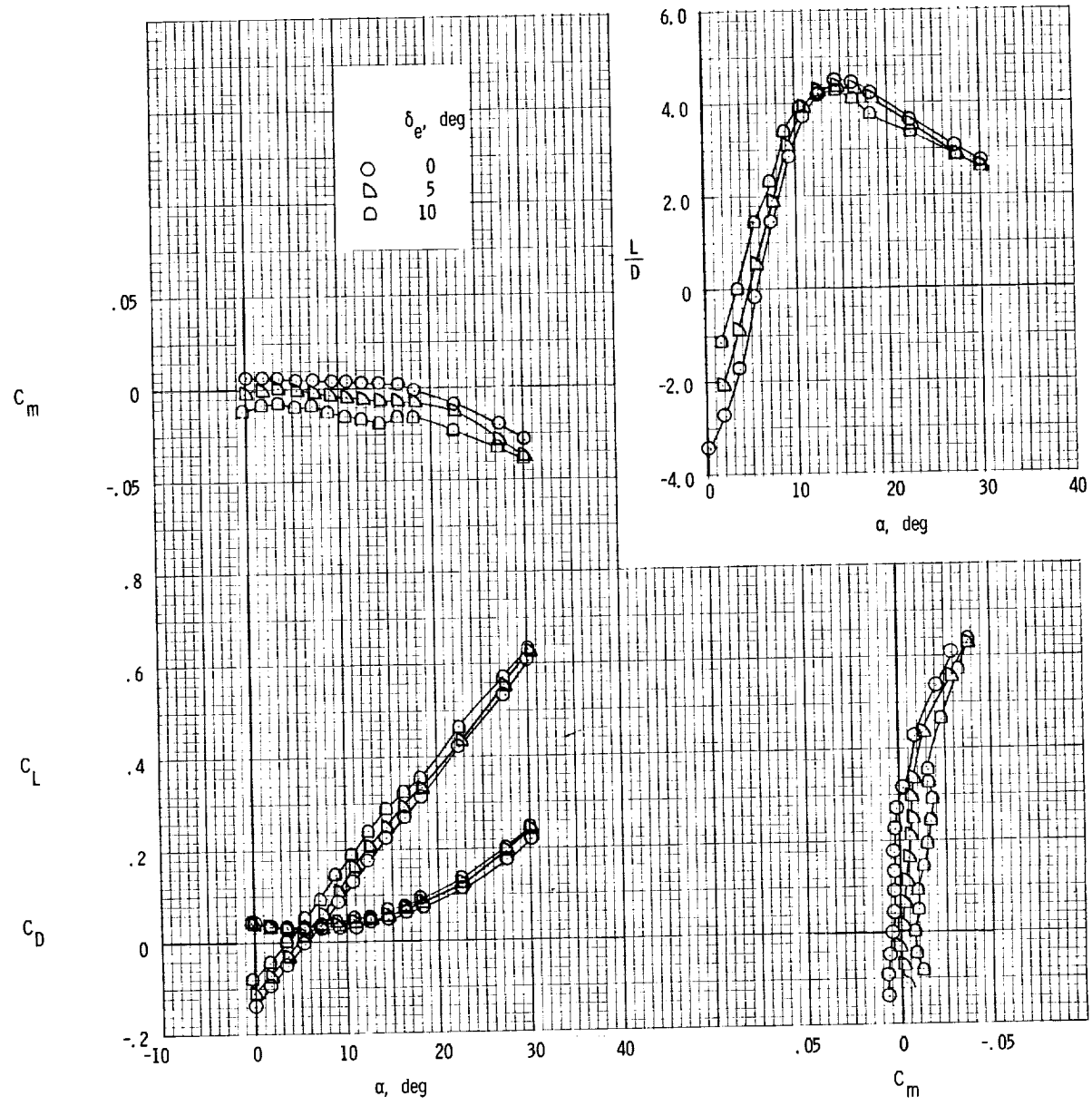

(a) Concluded.

Figure 7.- Continued.

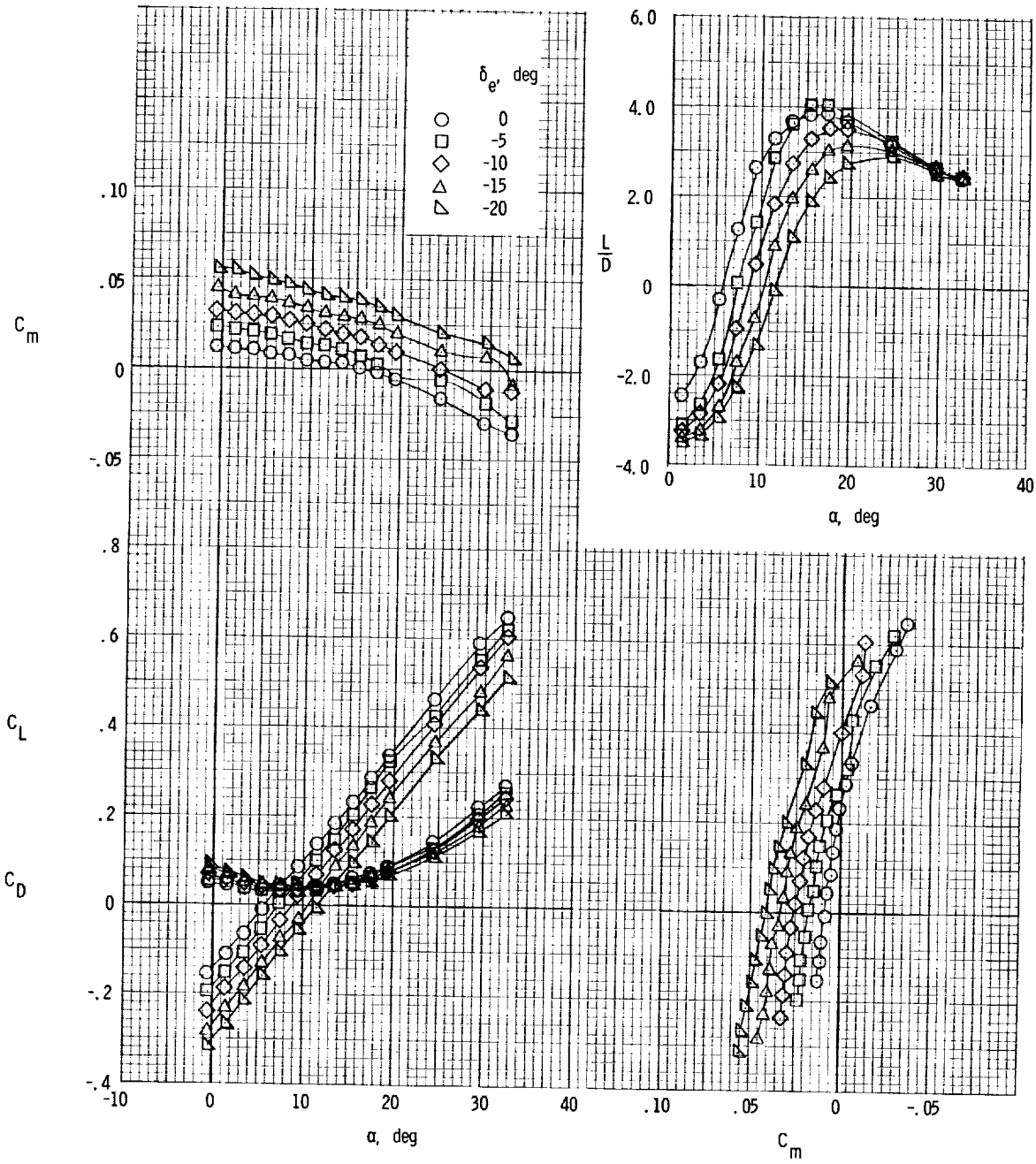

(b) Body with fin E_2.

Figure 7.- Continued.

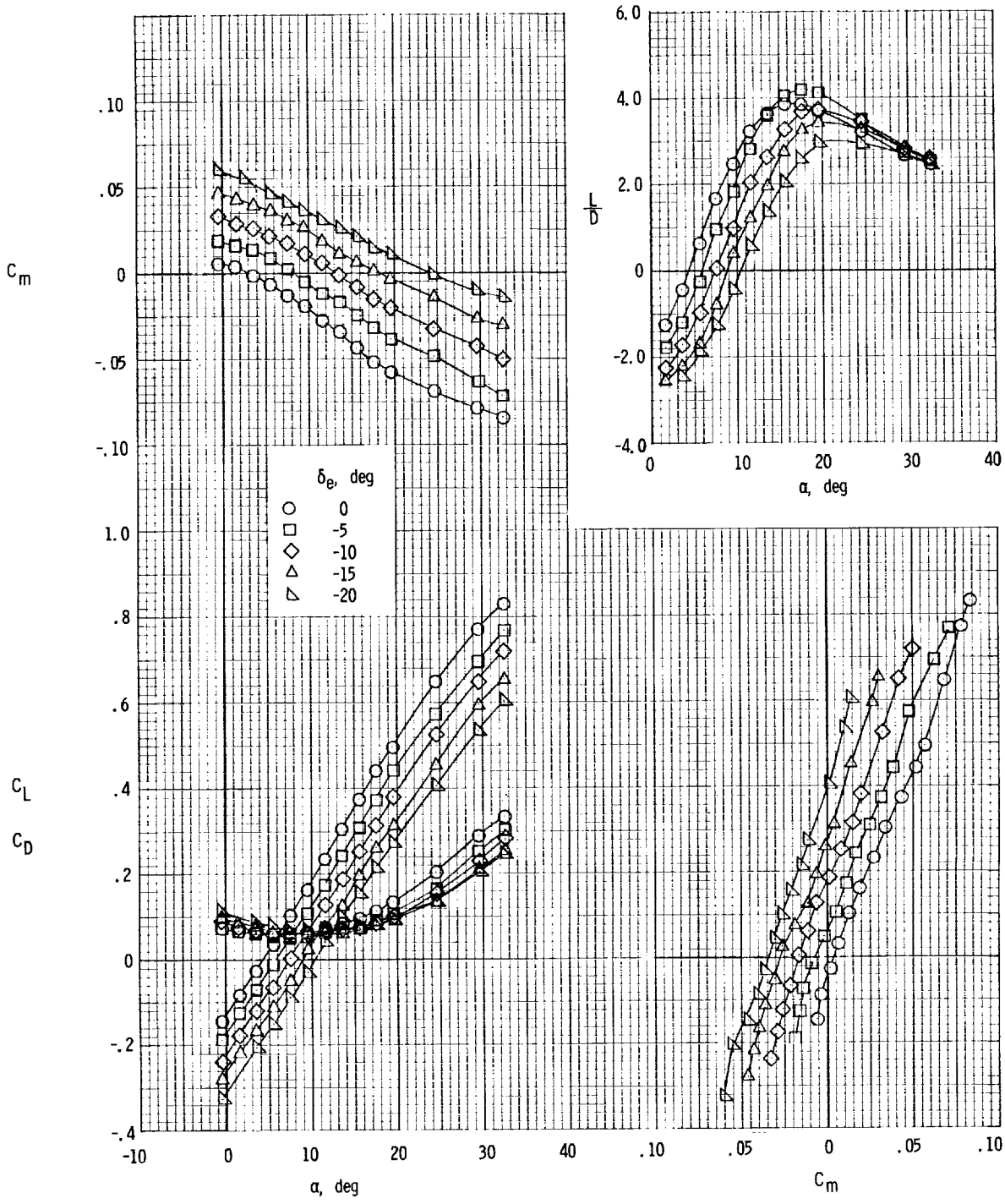

(c) Body with fins E_2 + I_4.

Figure 7.- Continued.

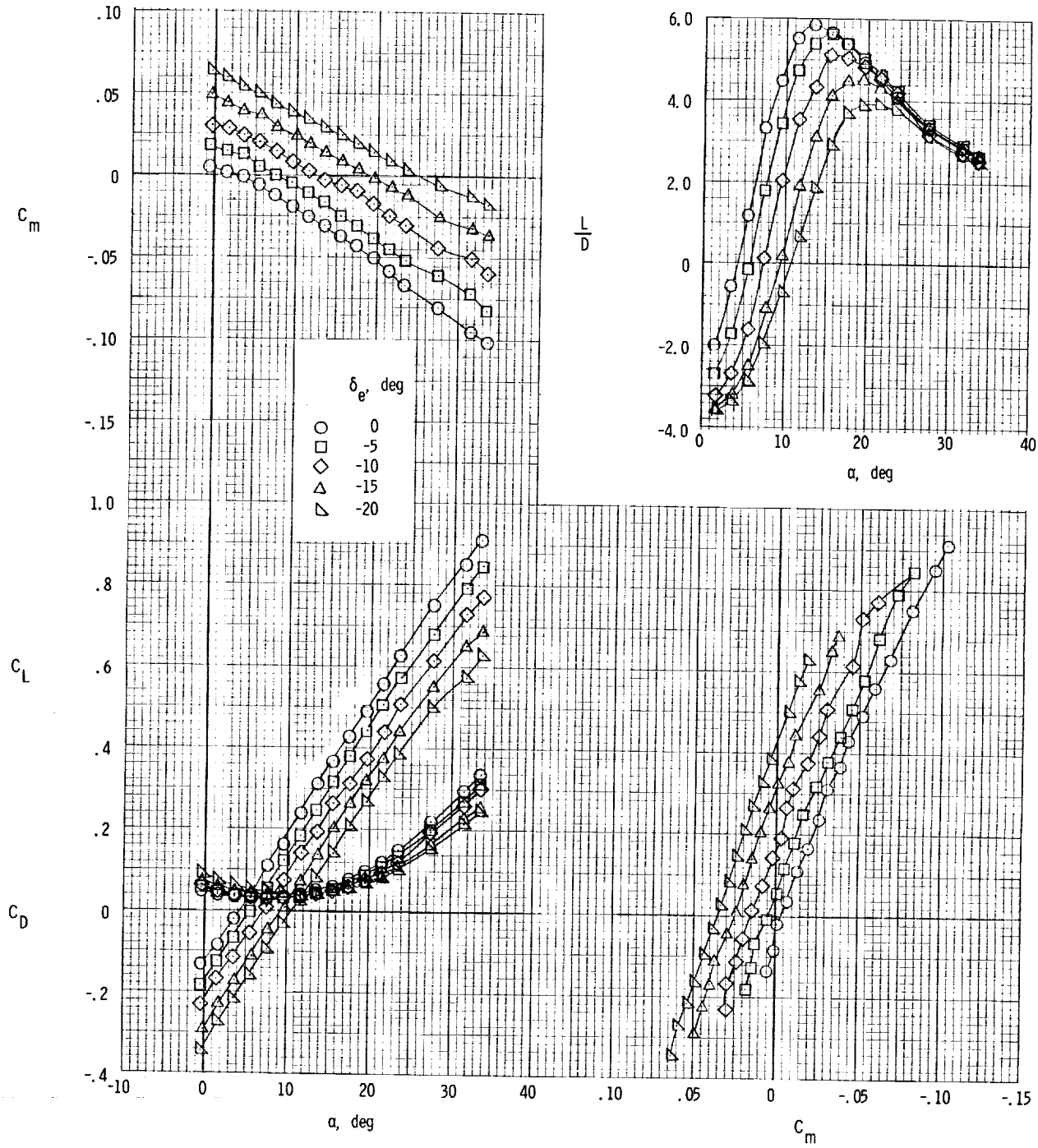

(d) Body with modified fins E_2 + I_4. $\theta = 4^o$.

Figure 7.- Continued.

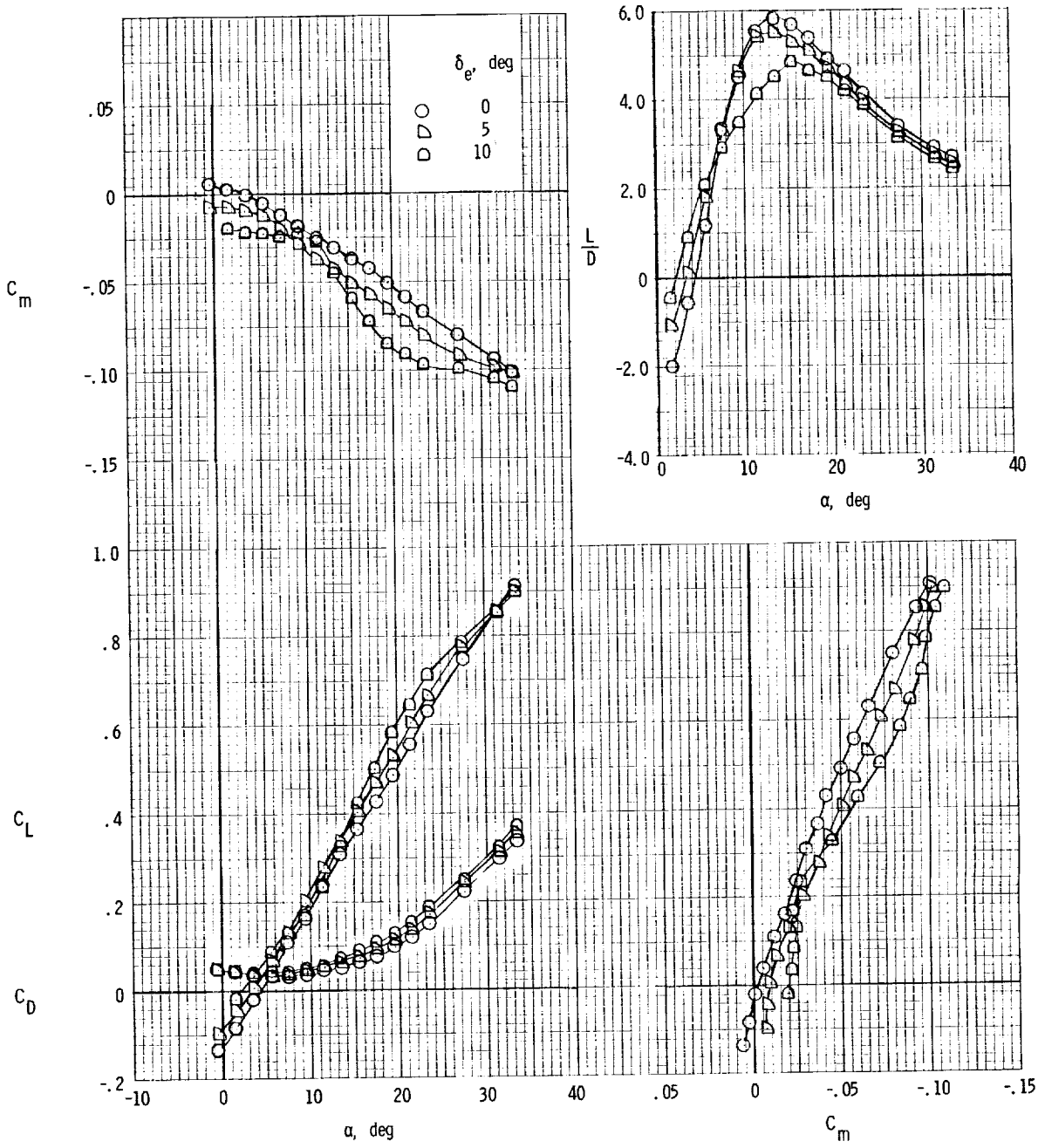

(d) Concluded.

Figure 7.- Concluded.

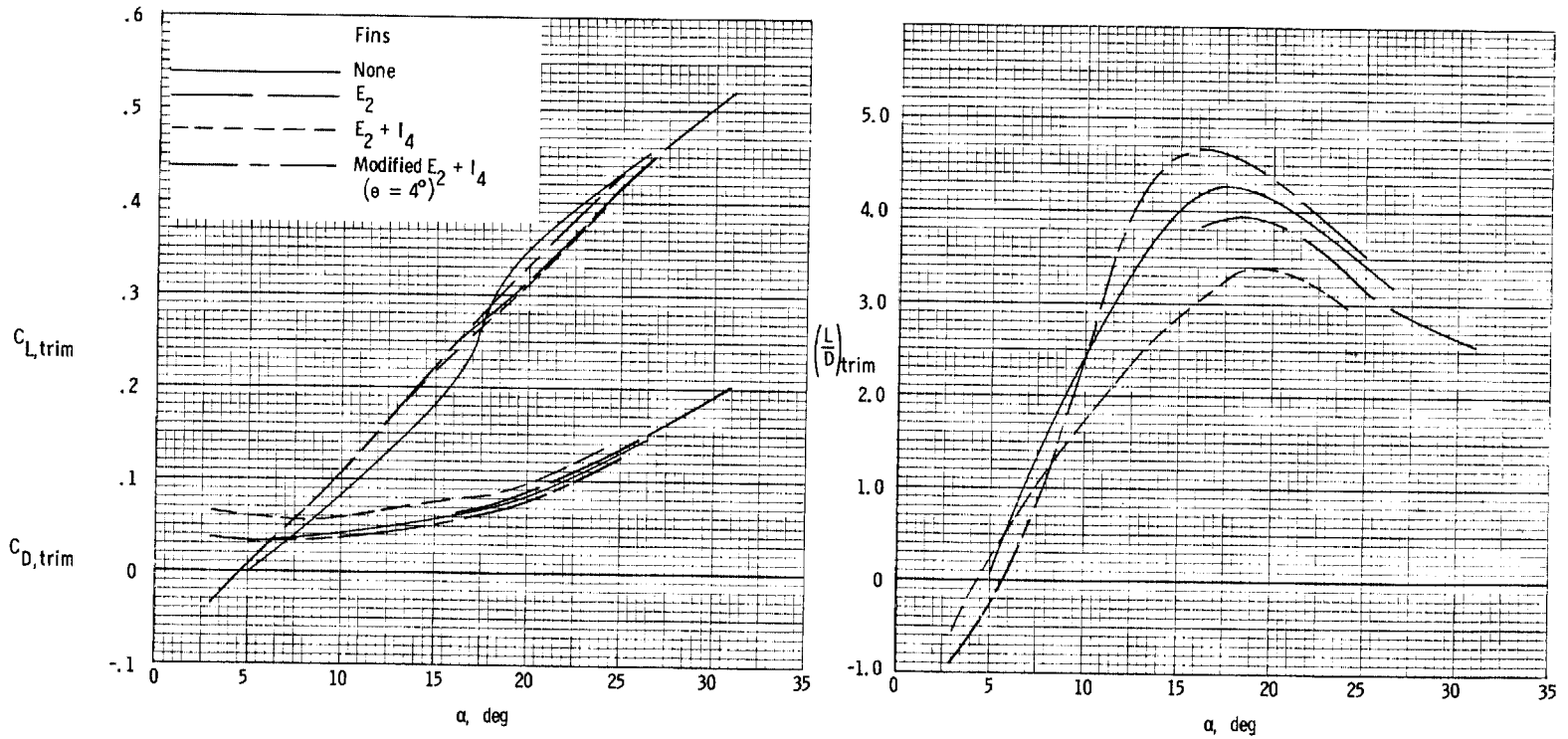

Figure 8.- Longitudinal trim characteristics of model.

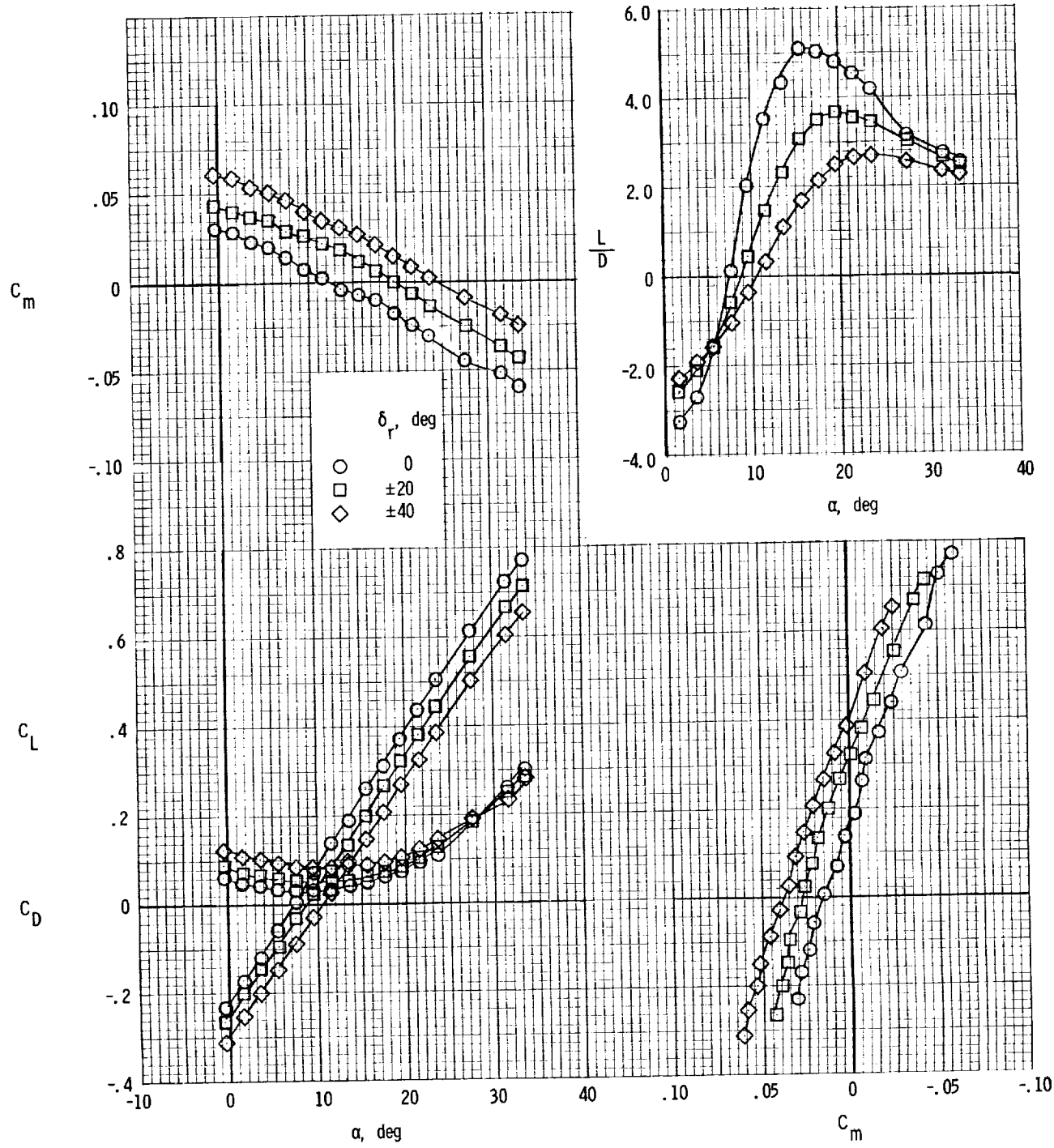

Figure 9.- Effect of speed-brake deflection on longitudinal characteristics of model with modified fins $E_2 + I_4$. $\delta_e = -10^0$; $\theta = 4^0$.

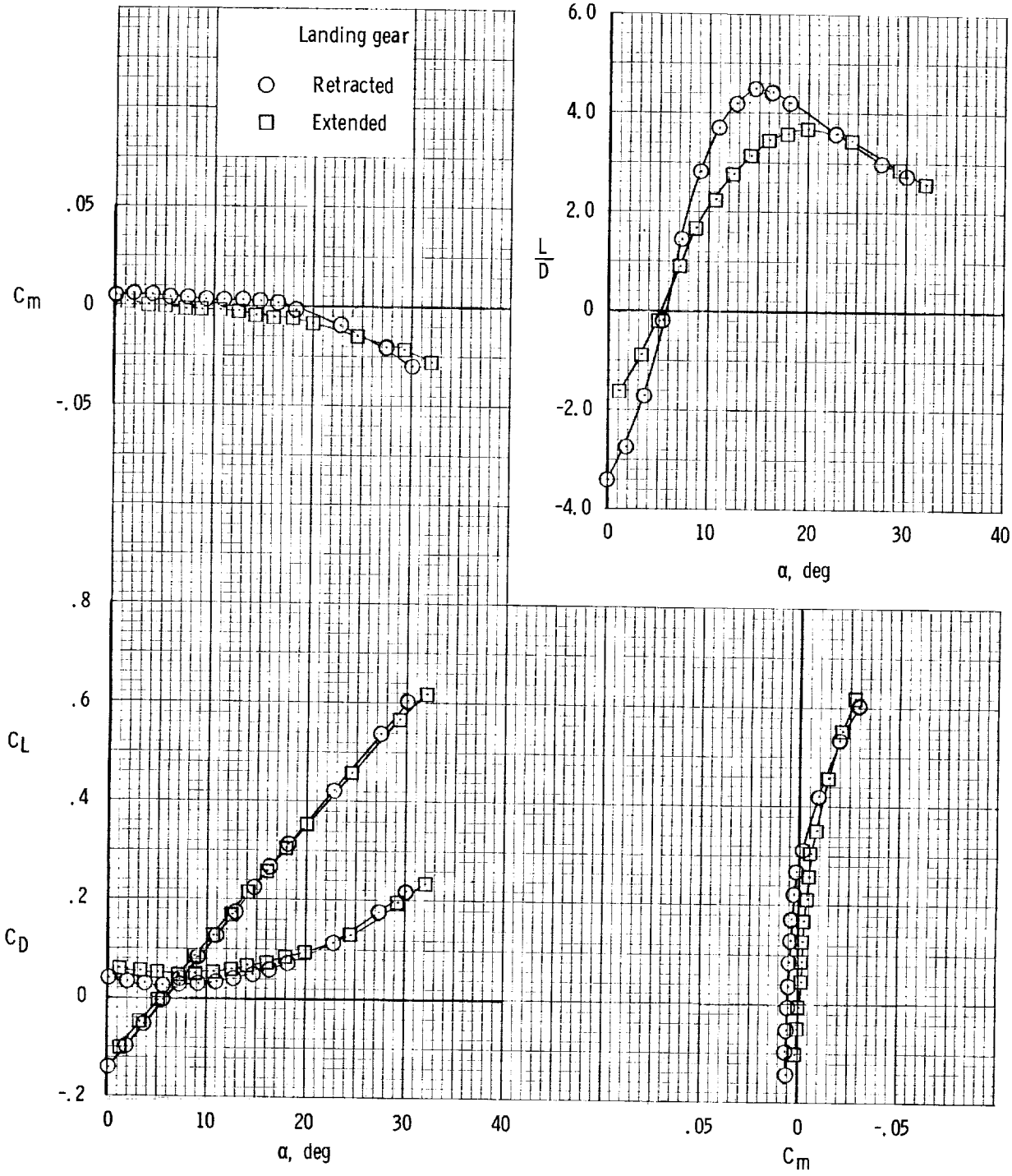

(a) Body alone.

Figure 10.- Effect of landing gear on longitudinal characteristics of model. $\beta = 0^0$; $\delta_e = 0^0$.

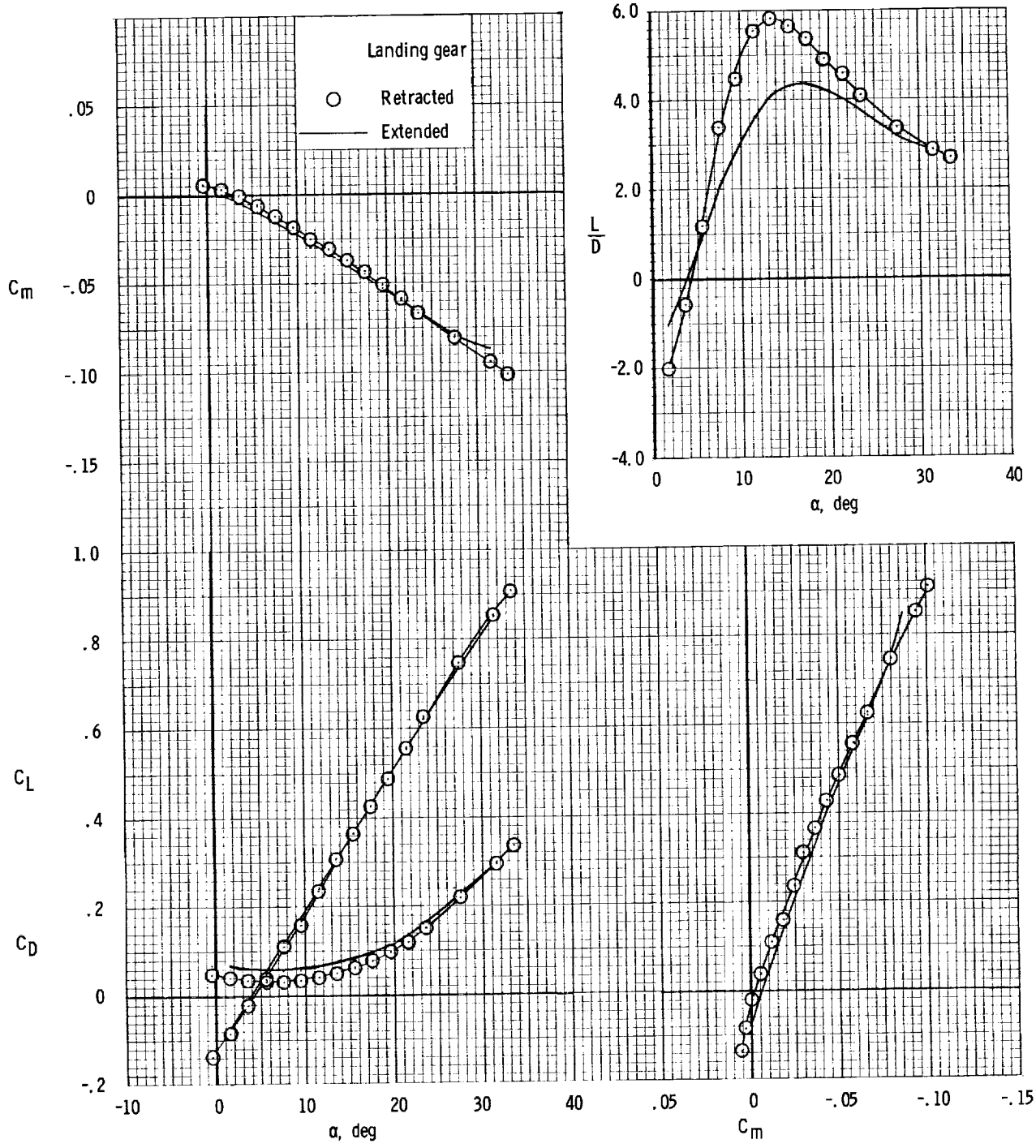

(b) Body with modified fins E_2 + I_4. $\theta = 4^0$.

Figure 10.- Concluded.

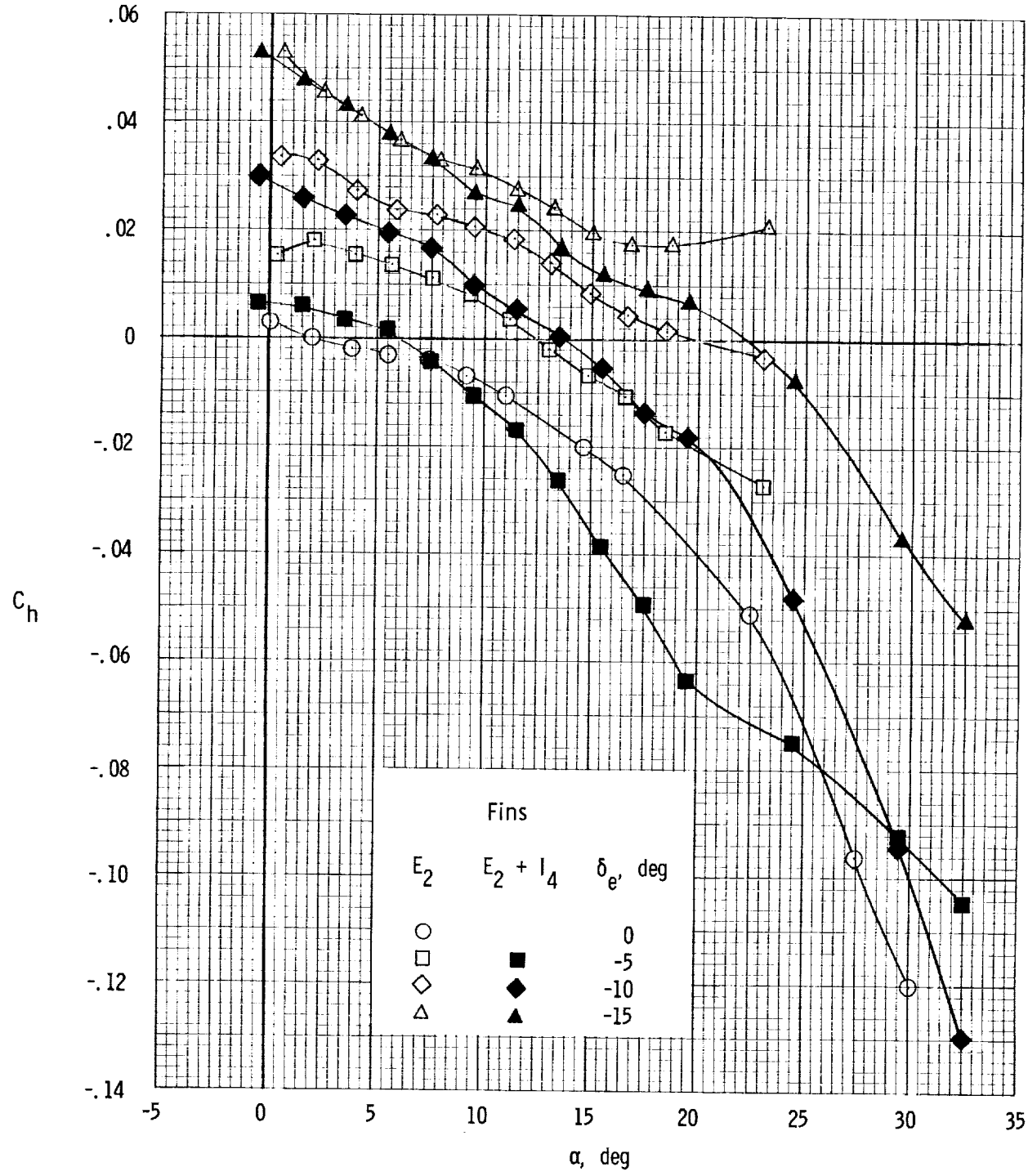

Figure 11.- Elevator hinge-moment characteristics of model.

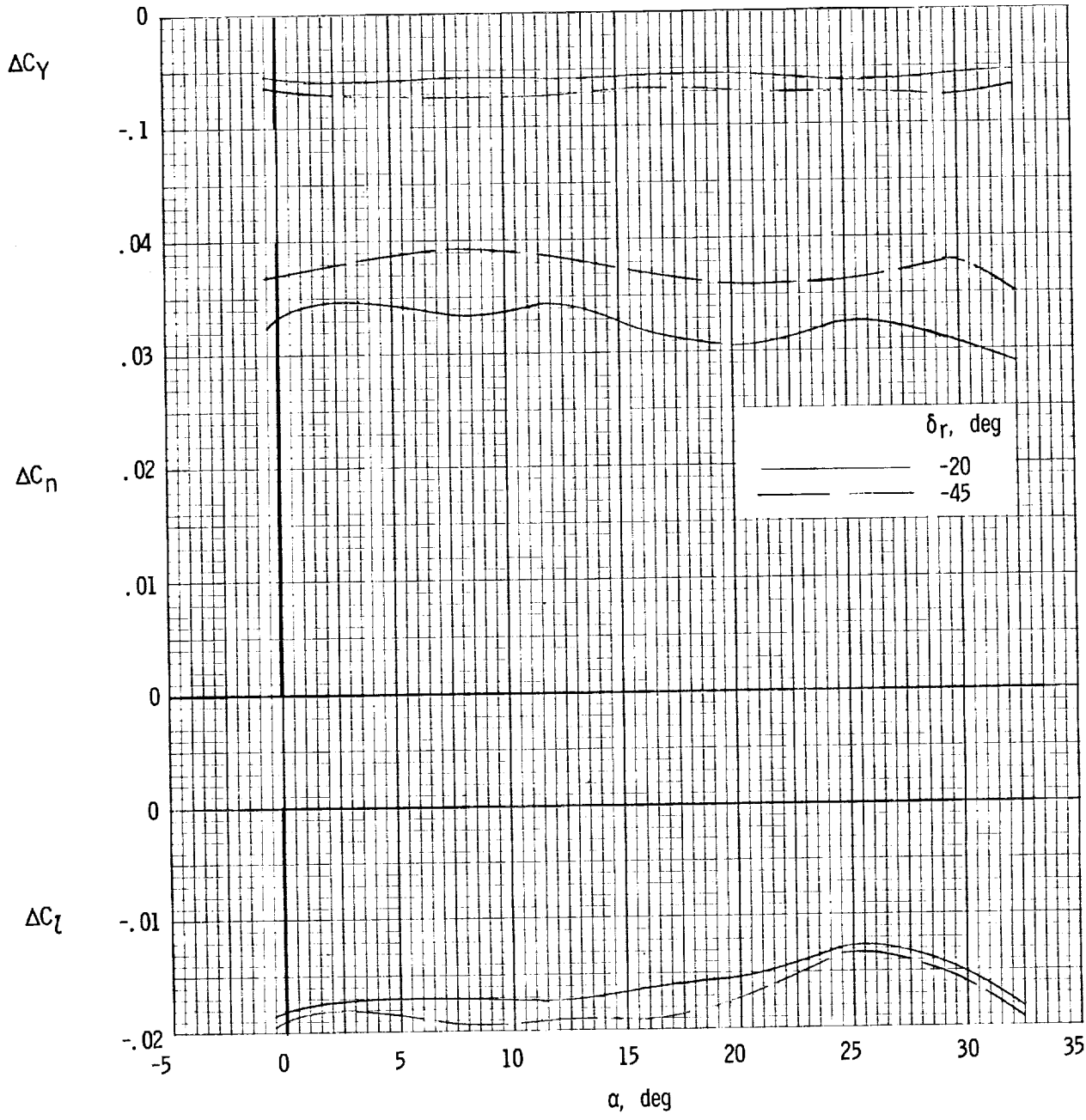

(a) Body with fin E_2.

Figure 12.- Effect of rudder deflection on lateral control characteristics of model.

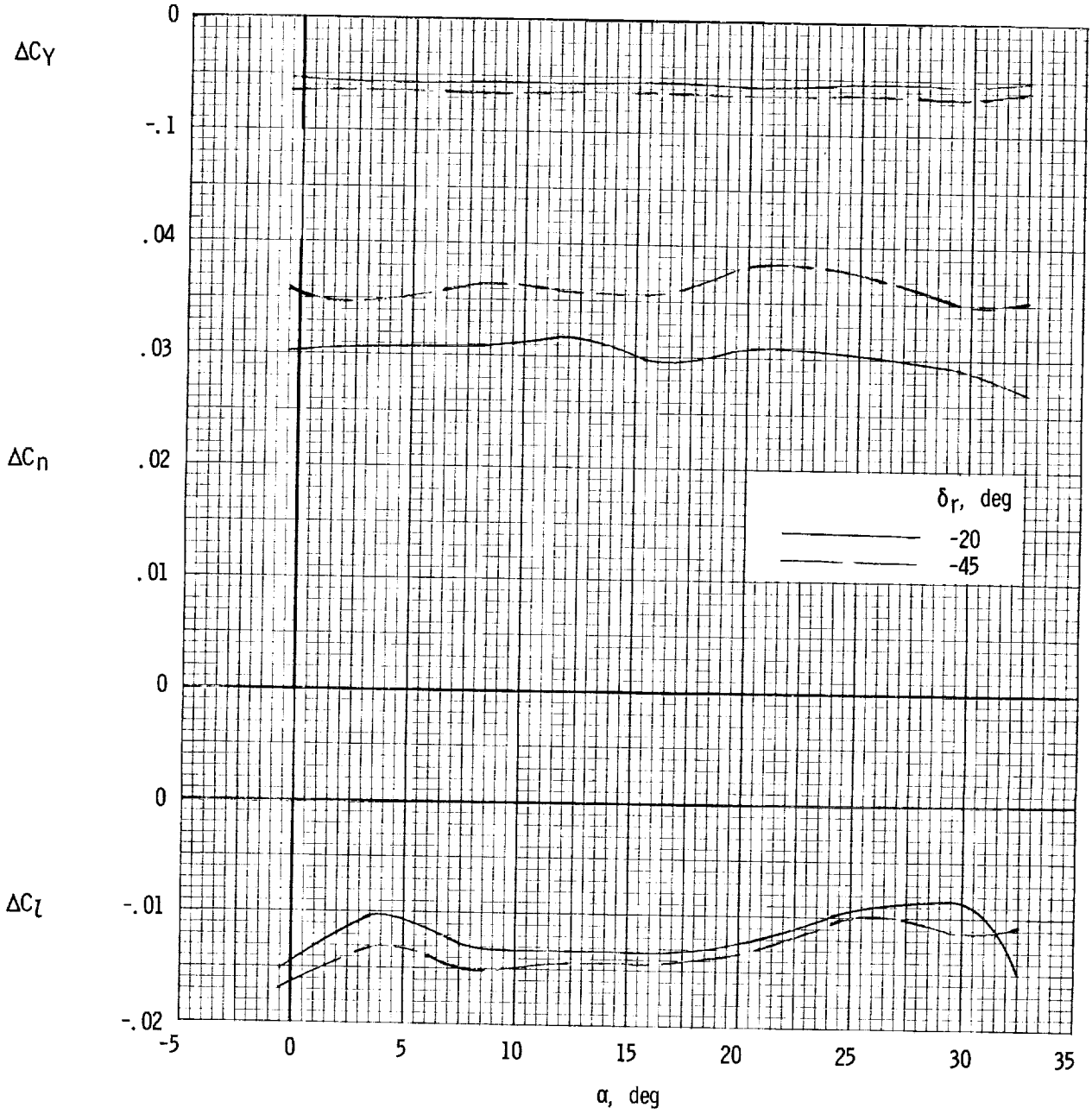

(b) Body with fins E_2 + I_4.

Figure 12.- Continued.

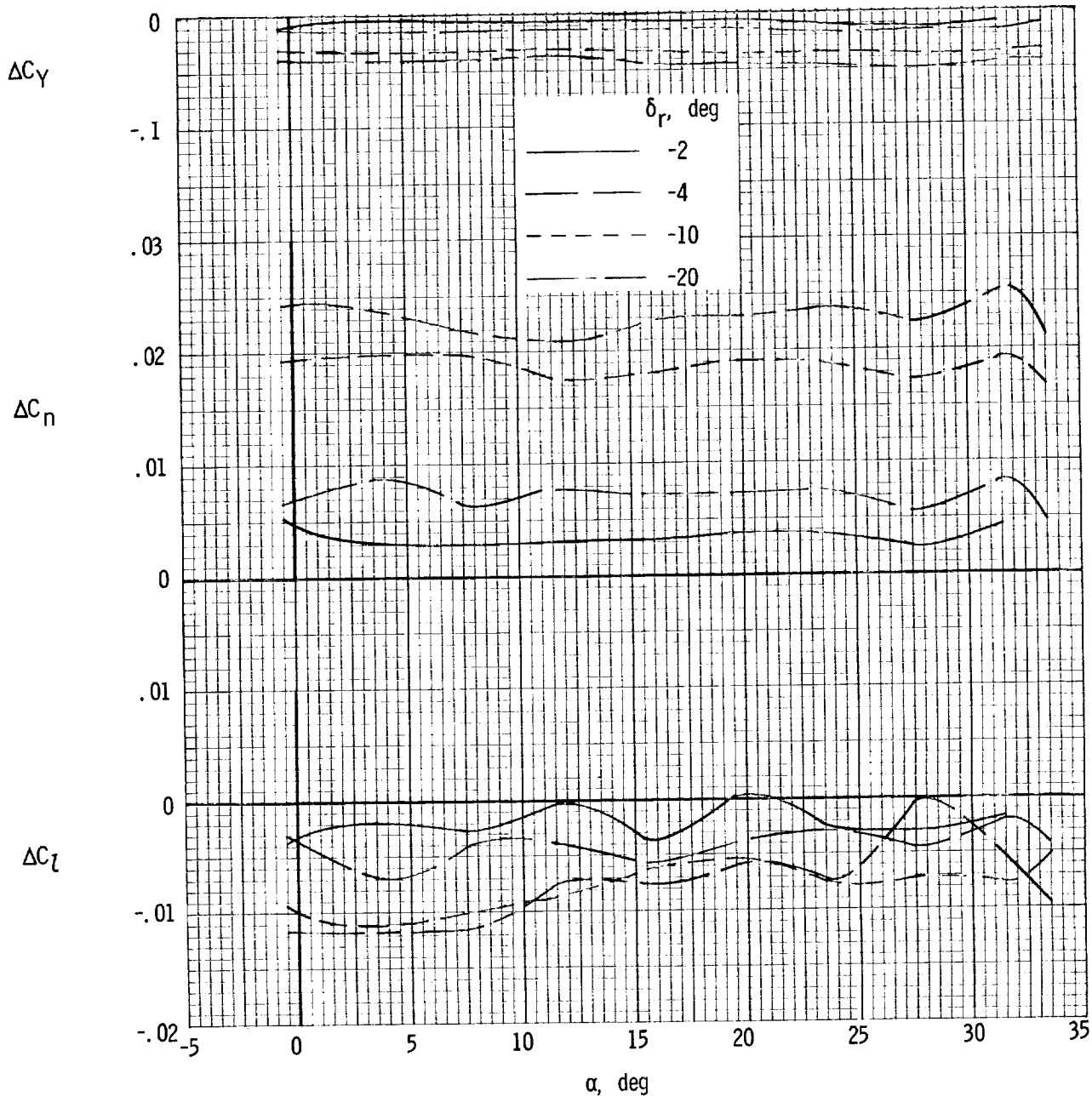

(c) Body with modified fins E_2 + I_4. $\theta = 4^o$.

Figure 12.- Concluded.

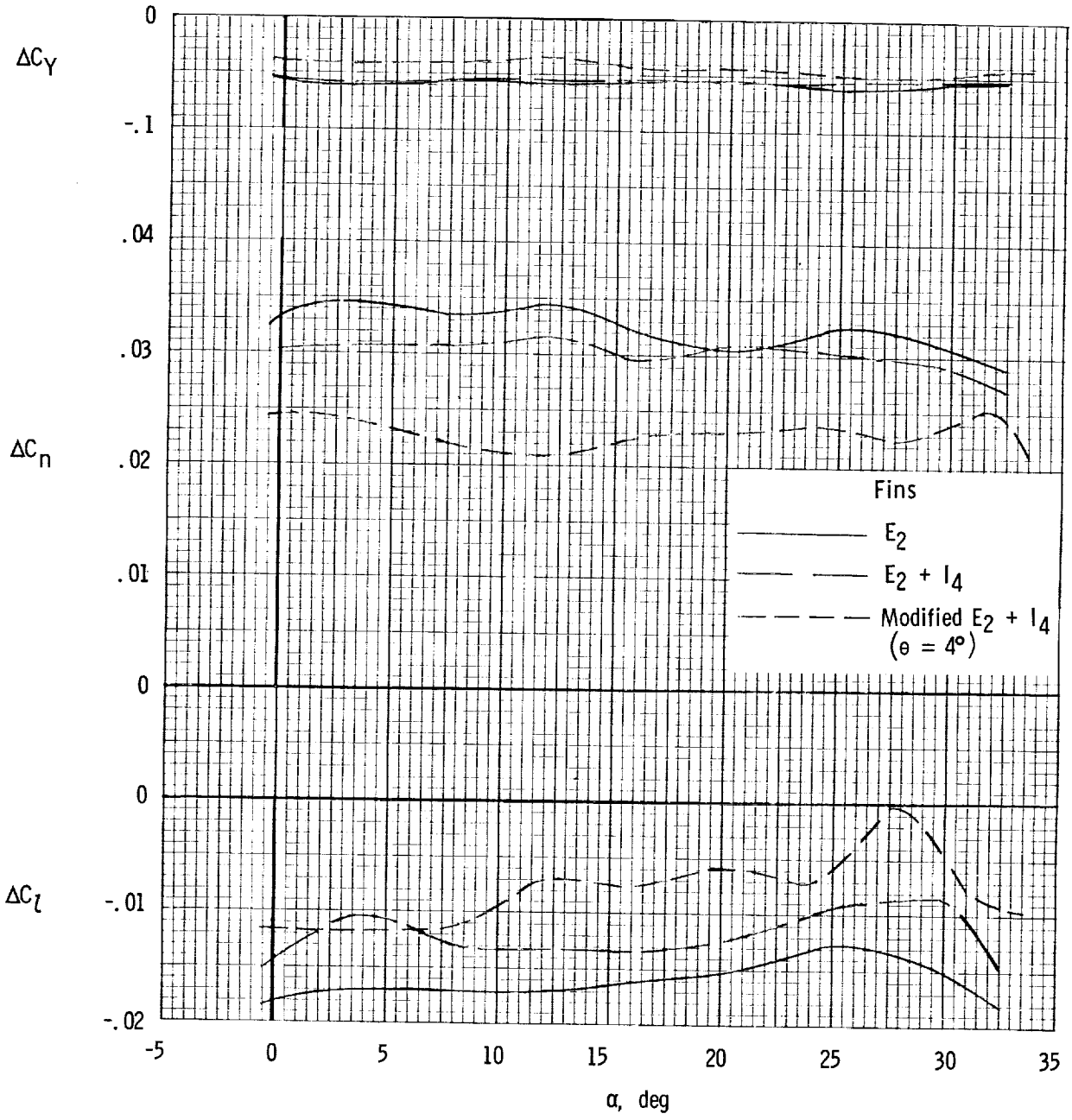

Figure 13.- Comparison of rudder effectiveness of model with various fin configurations. $\delta_r = -20^0$.

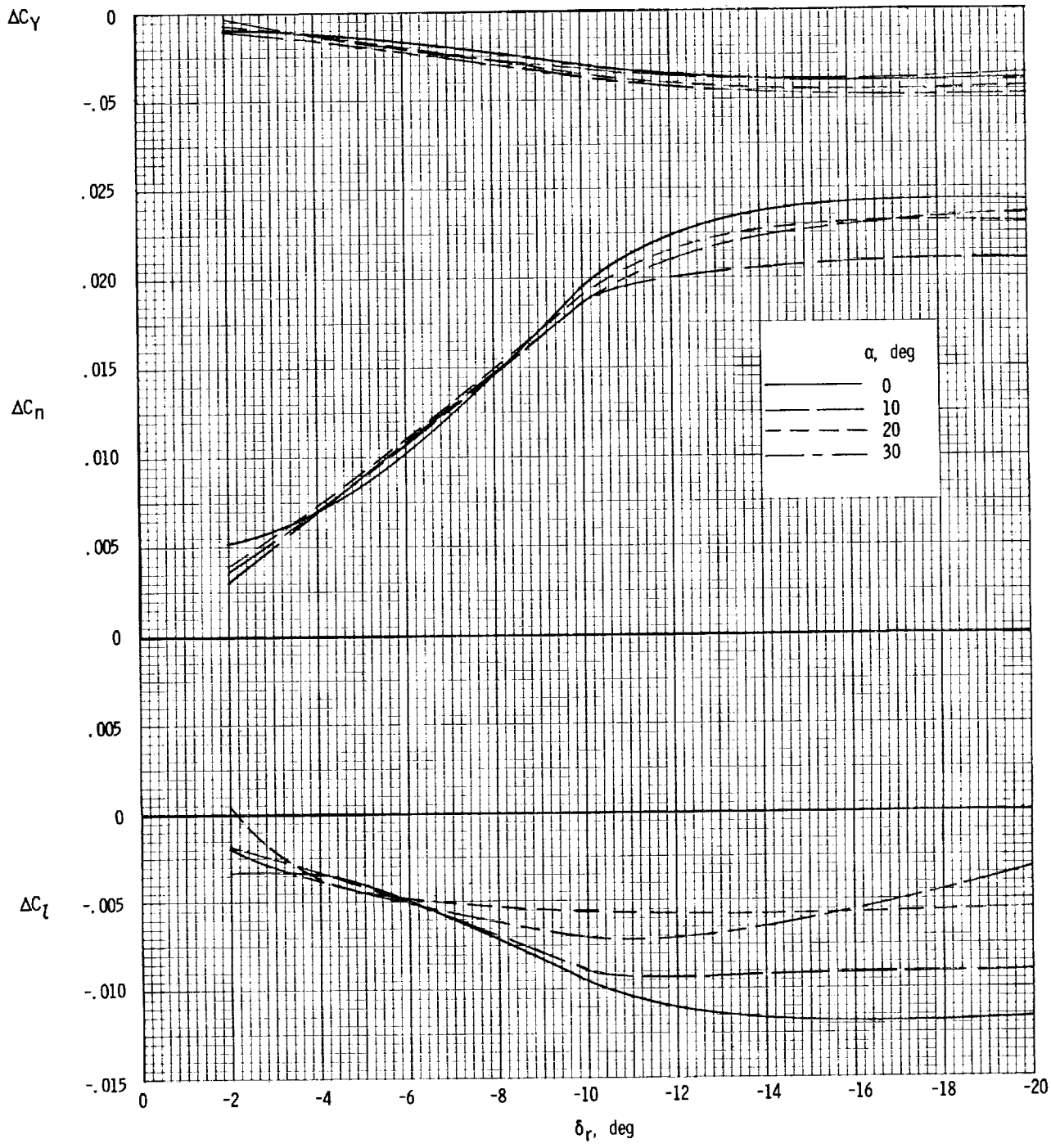

Figure 14.- Comparison of rudder effectiveness of model with modified fins E_2 + I_4 for various rudder deflection angles. $\theta = 4^0$.

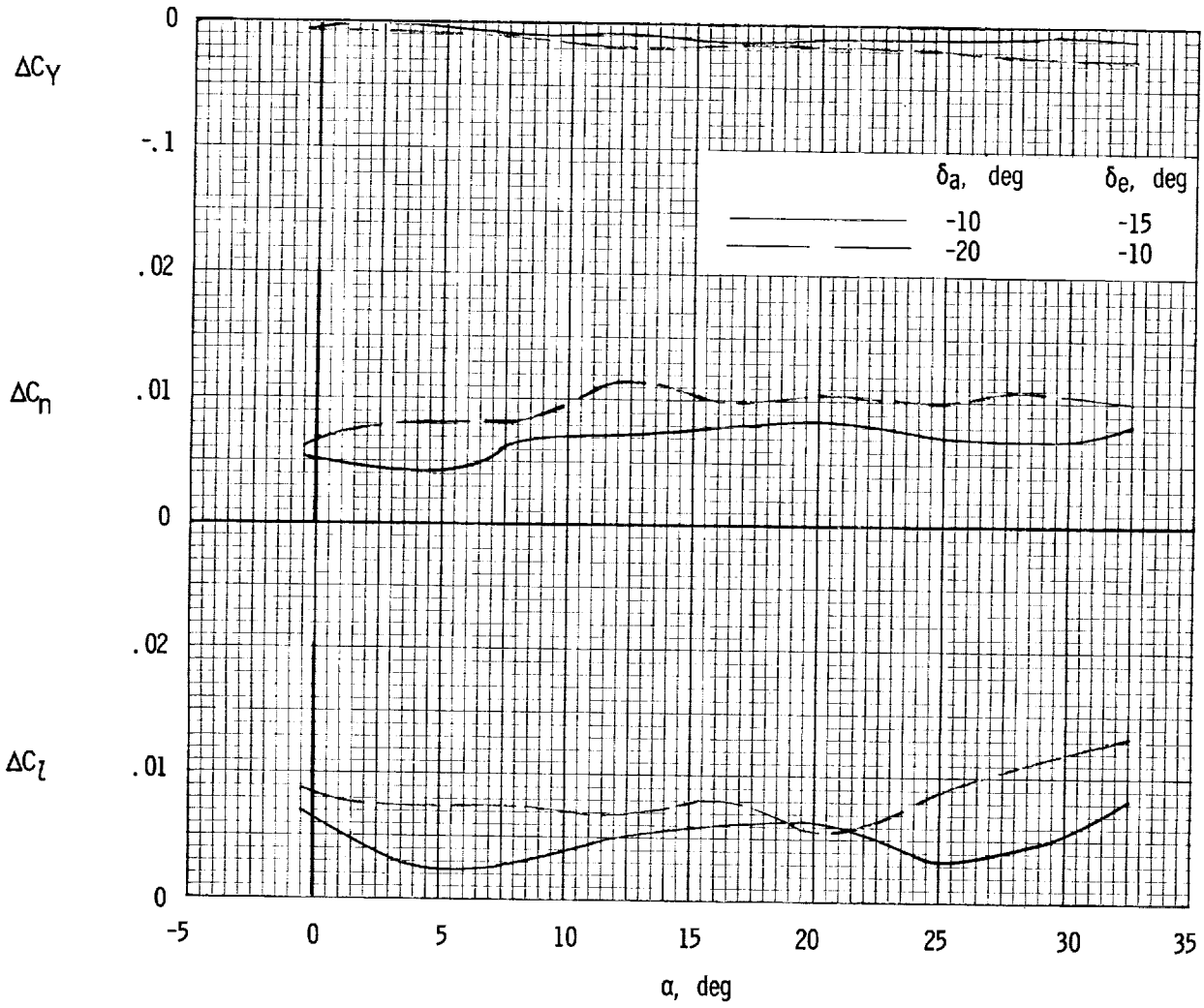

(a) Body with fin E_2.

Figure 15.- Effect of aileron deflection on lateral control characteristics of model.

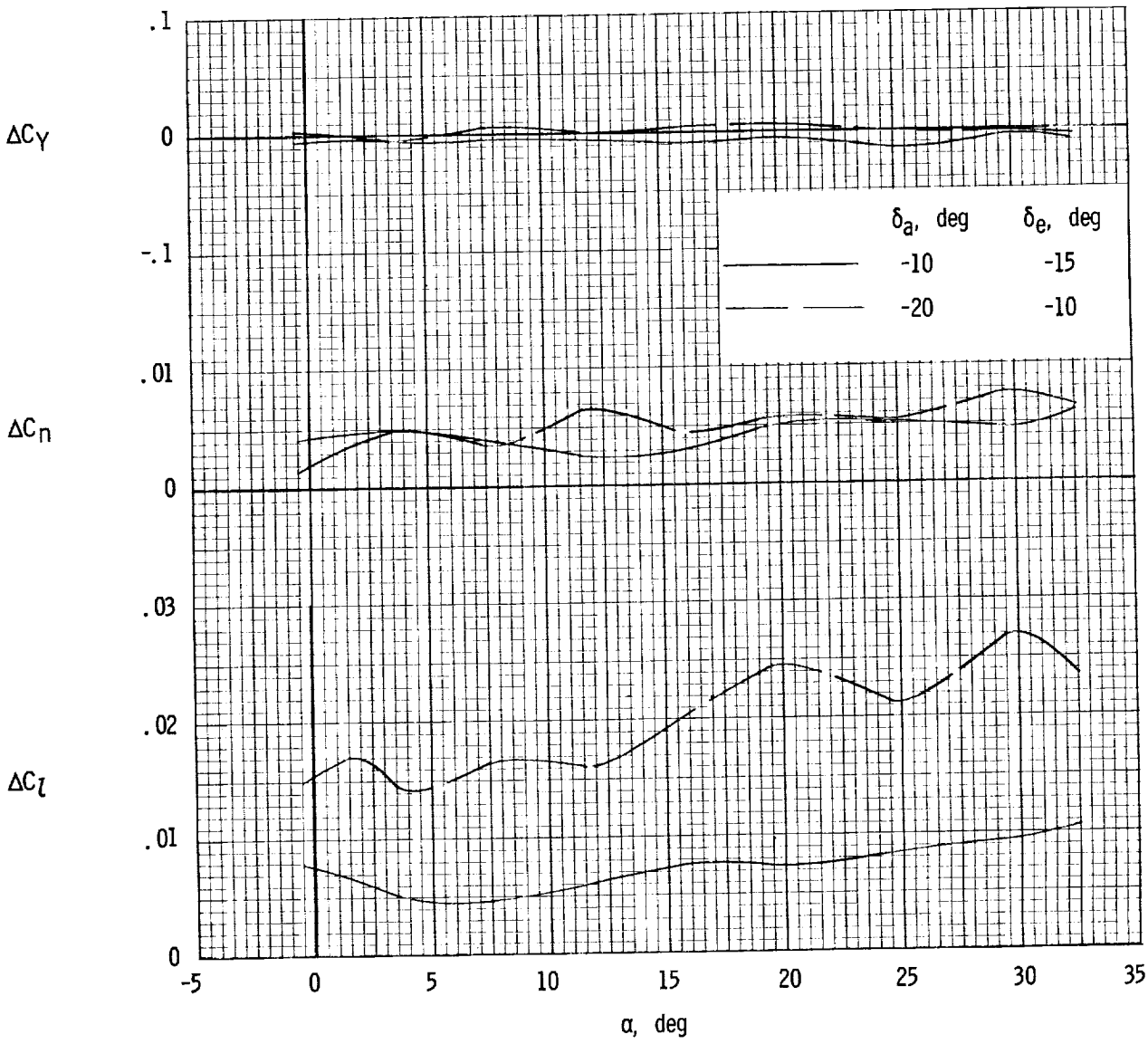

(b) Body with fins E_2 + I_4.

Figure 15.- Continued.

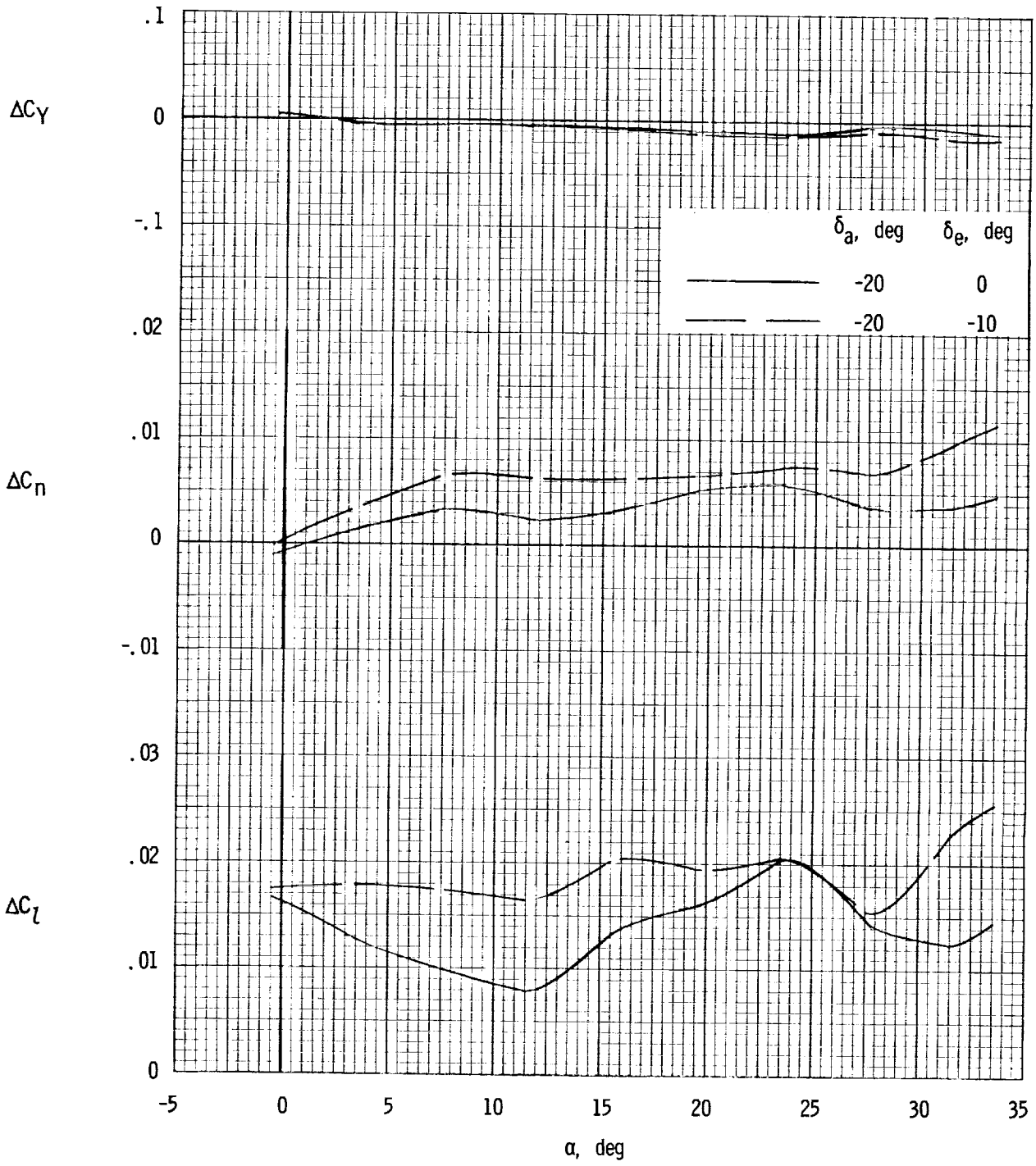

(c) Body with modified fins $E_2 + I_4$. $\theta = 4^o$.

Figure 15.- Concluded.

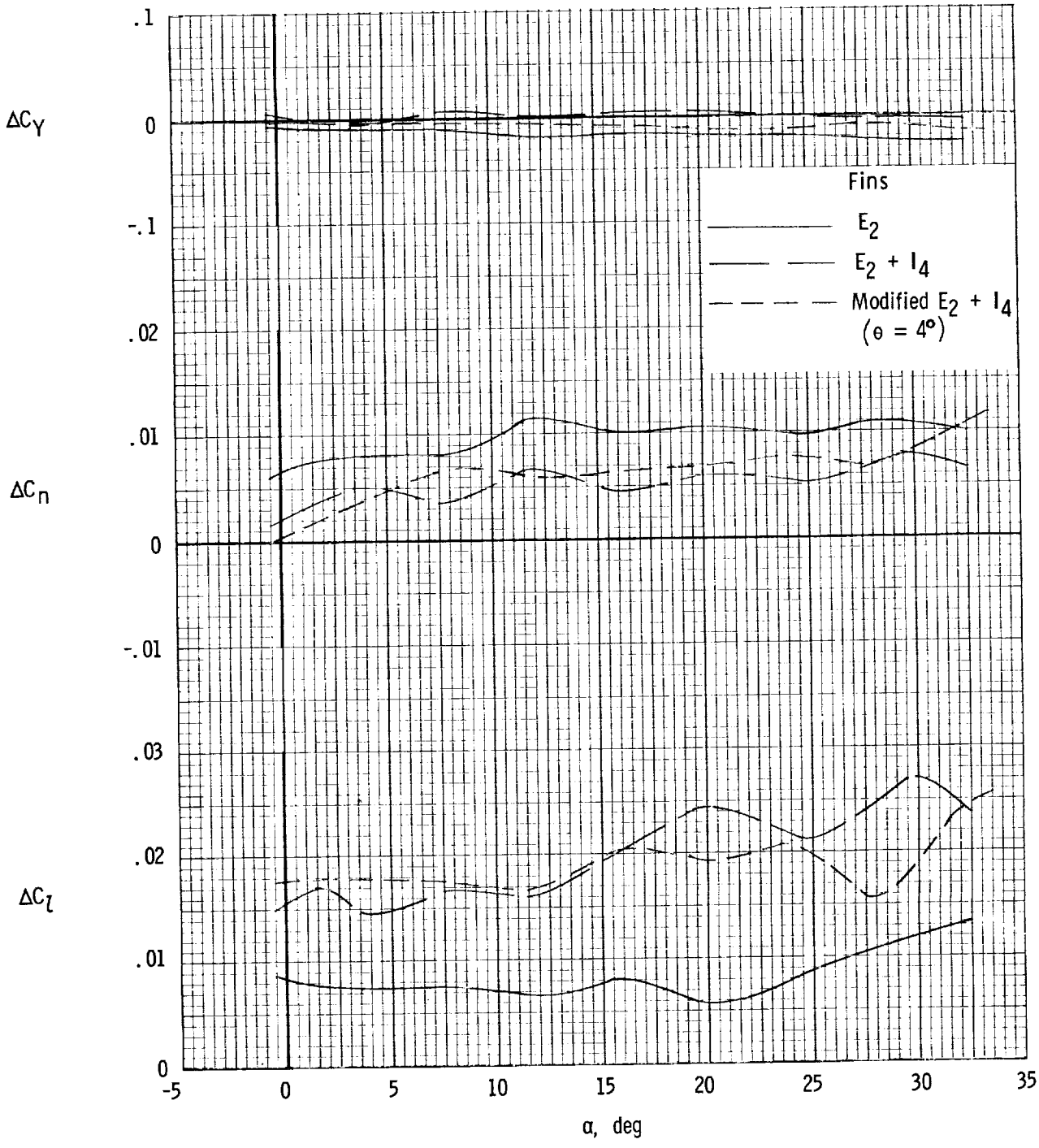

Figure 16.- Comparison of aileron effectiveness of model with various fin configurations. $\delta_a = -20^0$; $\delta_e = -10^0$.

[redacted]

[redacted]